Aus dem Medizinischen Zentrum für Operative Medizin

Klinik für Neurochirurgie

Geschäftsführender Direktor: Prof. Dr. Ch. Nimsky

des Fachbereichs Humanmedizin der Philipps-Universität Marburg

Purification and Functional Characterisation of Recombinant Human ADAM8 protease

Inaugural-Dissertation
zur
Erlangung des Doktorgrades der gesamten Humanmedizin
dem Fachbereich Medizin der Philipps-Universität Marburg
vorgelegt von

Xiangdi Yu

aus Hubei, China

Marburg, 2015

Angenommen vom Fachbereich Medizin der Philipps-Universität Marburg

am:

Gedruckt mit Genehmigung des Fachbereichs

Dekan: Prof. Dr. H. Schaefer

Referent: Prof. Dr. J.W. Bartsch

Korreferent: Prof.Dr.A.Pagenstecher

I. Table of content

Page

List of Figures

Abbreviation

ADAM	A Disintegrin and Metalloprotease
BB-94	Batimastat
BSA	Bovine serum albumin
℃	Celsius
CD	Cytoplasmic domain
CO_2	Carbon dioxide
CT1746	(N1-[2-(S)-(3,3-dimethylbutanamidyl)]-N4-hydroxy-2-(R)-[3-(4-chlorophenyl)-propyl] succinamide
Cys	cysteine-rich domain
DIS	Disintegrin domain
DMSO	Dimethylsulfoxide
DMEM	Dulbecco's modified eagle medium
FN	Fibronectin
FBS	Fetal bovine serum
h	hour
hEctoA8	human EctoADAM8
kDa	Kilo Dalton
MP	metalloprotease domain
min	Minute
ml	Milliliter
NaCl	Sodium chloride
PFA	Paraformaldehyde
PBS	Phosphate buffered saline
Pro	prodomain
SDS	Sodium dodecylsulphate
SDS-PAGE	SDS-Polyacrylamide gel electrophoresis
TEMED	N,N,N',N'-Tetramethylethylenediamine
Tris	Tris-(hydroxy methyl)-amino methane
TM	Transmembrane domain

1. Introduction

1.1 A Disintegrin and Metalloprotease (ADAM) family member-ADAM8

ADAM8 (also known as CD156a, MS2) was originally cloned from a murine macrophage cDNA library and described as a novel cell surface protein mainly expressed on monocytes[1]. ADAM8 has the typical structure of an ADAM family member consisting of an inhibitory prodomain (Pro), a metalloprotease domain (MP), a disintegrin domain (DIS), a cysteine-rich domain (Cys), a EGF-like domain (EGF) followed by the transmembrane (TM) and the cytoplasmic domain (CD)[2].

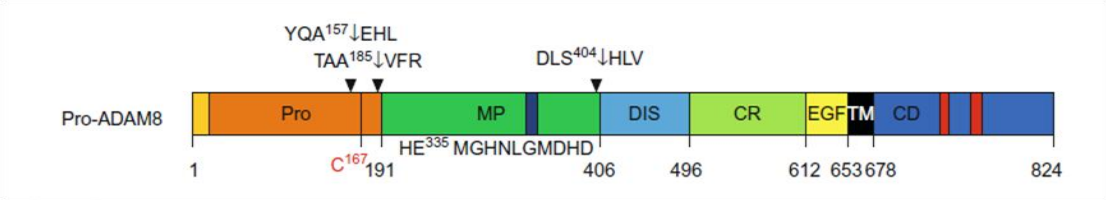

Figure 1: Domain organisation of ADAM8

Protein domains are drawn to scale, and the amino acid positions are given below. Abbreviations for domains: Pro, prodomain; MP, metalloprotease; DIS, disintegrin; CR, cysteine-rich; EGF, EGF-like domain; TM, transmembrane domain; CD, cytoplasmic domain. The extracellular ectodomain of ADAM8 (EctoA8) consists of CR, DIS and MP with or without Pro. Scheme adapted from Koller et al[2].

ADAM8 is produced as an inactive pro-protein (pro-ADAM8). The mature active form is activated by removal of the prodomain. In contrast to most other proteolytically active ADAMs, ADAM8 contains a non-canonical furin consensus sequence (RETR as opposed to RX (K/R) R) in the hinge region between the Pro and MP domain. Instead of furin-mediated cleavage, the Pro domain is removed by an autocatalytic mechanism[3]. In addition to its proteolytic activity, ADAM8 DIS domain contains an integrin binding loop with a central KDM motif as opposed to an integrin binding RGD motif present in the analogous position of human ADAM15. It was shown that the recombinant DIS/Cys/EGF (DCE) domain of ADAM8 mediates cell adhesion with ADAM8-expressing cells[3].

ADAM8 was originally described in relation to its involvement in inflammatory

processes[4] and subsequently in many systems of the body[2]. Recently, additional work demonstrated a role of ADAM8 in tumors, in particular in adenocarcinomas. In pancreatic ductal adenocarcinoma (PDAC) patient samples, high ADAM8 expression levels have been associated with a poor patient prognosis with regard to survival and metastatic spread[5]. This correlation was also observed in high-grade glioma[6], lung adenocarcinoma[7], prostate cancer[8] and more recently in squamous head and neck cell carcinoma[9], medulloblastoma[10] and osteosarcoma[11] suggesting that ADAM8 plays an active role in tumor progression, underlining the need to understand the functional role of ADAM8 in tumor biology. Up to now, ADAM8 has been associated with increased tumor cell migration, invasion and metastasis via a combination of catalytic, adhesion and cell signaling functions[5, 6]. From a very recent study it is clear that ADAM8 interacts with integrin β1 on the cell surface and activates intracellular signaling via p-ERK1/2 and PI3K and Akt signaling[12].

Recombinant ADAM8 has catalytic activity towards a number of peptide substrates[13-16]. From these peptide sequences, cleavage *in vivo* was demonstrated for five substrates: Amyloid Precursor protein, APP [14]; low affinity IgE receptor, CD23 [15]; L-selectin[17]; tumor necrosis factor alpha receptor 1, TNF-R1[18] and P-Selectin Glycoprotein Ligand-1 (PSGL-1)[19]. In particular, for TNF-R1, the findings demonstrate an additional neuroprotective role for ADAM8 under neurodegeneration conditions via TNF-R1 shedding: *Adam8* deficiency in mice with motoneuron degeneration (MND) (*Adam8*$^{-/-}$ *wr/wr*) showed an aggravated disease phenotype with survival, earlier onset, even more dramatic motor neuron loss in the spinal cord and increased reactive gliosis. Under neurodegenerative conditions in MND mice, TNF-α is activated in neurons, astrocytes and microglia and induces apoptosis *via* the TNF-R1 pathway. Shedding of TNF-R1 by ADAM8 produces the soluble form of TNF-R1, which binds TNF-α, thus desensitising cells to its apoptotic action. It was shown that TNF-R1 shedding was completely abolished in *Adam8*$^{-/-}$ *wr/wr* mice thus negatively affecting neuronal survival. From this study it was concluded that ADAM8 is an inflammation-induced 'sheddase' for TNF-R1 with neuroprotective effects in CNS pathology[18]. More recent work demonstrates an important role for ADAM8 in

elimination of injured muscle fibers prior to skeletal muscle regeneration: Skeletal muscle of dystrophin-null mice, an animal model for Duchenne Muscular Dystrophy, deteriorates by the lack of ADAM8, which is characterized by increased area of muscle degeneration and increased number of necrotic and calcified muscle fibers. ADAM8 is highly expressed in neutrophils. Upon cardiotoxin-induced skeletal muscle injury, neutrophils invade into muscle fibers through the basement membrane and form large clusters in wild type, but not in *Adam8*$^{-/-}$ mice, although neutrophils of latter infiltrate into interstitial tissues similarly to those of wild type mice, whereas expression of PSGL-1 on the surface of neutrophils remains higher in *Adam8*$^{-/-}$ than in wild-type mice. Thus, ADAM8-dependent ectodomain shedding of PSGL-1 could contribute to the removal of cell surface PSGL-1 of neutrophils after their infiltration[19].

In order to characterise ADAM8 function *in vitro*, a soluble ectodomain lacking the transmembrane and the cytoplasmic domains should be produced. This human EctoADAM8 (hEctoA8) protein consists of the prodomain, metalloprotease domain (MP), a disintegrin domain (DIS), a cysteine-rich domain (Cys) and a EGF-like domain (EGF), whilst removal of the prodomain by autocatalysis leads to the active form of hEctoA8[3]. Like the full-length ADAM8, hEctoA8 contains the catalytic consensus sequence HEXXHXXGXXHD in the metalloprotease domain and is therefore predicted to be proteolytically active[20]. Up to now, functional studies on ADAM8 *in vitro* were hampered by the lack of sufficient quantities of folded, biologically active, and purified recombinant forms of hEctoA8.

Thus, in the study presented here, we propose to express and purify the recombinant ectodomain of human ADAM8 (hEctoA8) protein from supernatants of transfected HEK cells and investigate the biological properties of ADAM8 with respect to substrates, cell adhesion and signaling.

1.2 CD23

CD23 was one of the first described substrates for ADAM8 with implications for inflammatory and allergic disease. CD23, also known as Fc epsilon RII, or FcεRII, is the "low-affinity" receptor for IgE, an antibody isotype involved in allergy and resistance to parasites, and is important in regulation of cellular IgE levels. Unlike many of the antibody receptors, CD23 is a C-type lectin. It is found on mature B cells, activated macrophages, eosinophils, follicular dendritic cells, and platelets.

Two isoforms of CD23 exist which are CD23a and CD23b. Whereas CD23a is present on follicular B cells, CD23b requires IL-4 to be expressed on T-cells, monocytes, langerhans cells, eosinophils, and macrophages[21]. CD23 is known to have a role in mediating antibody feedback regulation. Antigen that enters the blood stream is captured by antigen specific IgE antibodies. The IgE immune complexes that are formed bind to CD23 molecules on B cells, and are transported to the B cell follicles of the spleen. The antigen is then transferred from CD23+ B cells to CD11c+ antigen presenting cells. The CD11c+ cells in turn present the antigen to CD4+ T cells, which can lead to an enhanced antibody response[22].

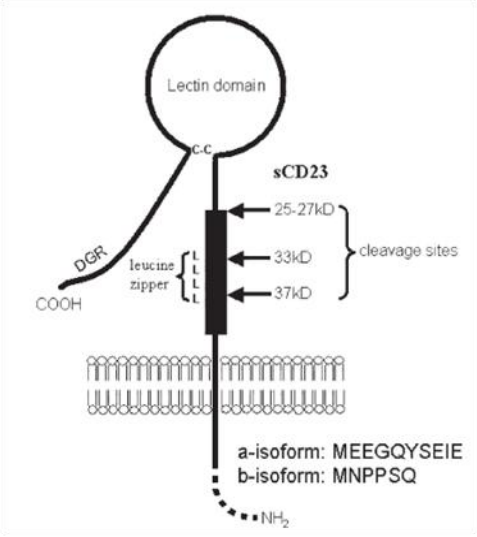

Figure 2: Schematic representation of human CD23

Two isoforms have been described for human CD23 which differ only in the N-terminal sequence. Some important structural features indicated are the leucine-zipper, mediating formation of homotrimers, the C-type lectin domain, with the ability to bind either the IgE-protein portion or carbohydrate chains containing a terminal galactose, the protease cleavage sites giving rise to sCD23 molecules of the indicated fragment sizes, and an inverse RGD sequence. RGD sequences have a function in the interaction of integrins with their ligands[23].

CD23 is cleaved from the cell surface to generate a number of soluble forms that have been shown to be elevated in a number of diseases such as asthma, rheumatoid arthritis, and inflammatory bowel disease[24]. Soluble forms of CD23 play an important role in the up-regulation of IgE synthesis by interaction with B cells[25], as well as promoting the induction of inflammatory cytokines by macrophage[24]. ADAM8 can contribute to shedding of CD23 to form soluble CD23[15], though shedding was not reduced in ADAM8 deficient mice [26] demonstrating that ADAM8 is not a constitutive shedding enzyme for CD23, a role assigned to ADAM10. It seems plausible that ADAM8 is amplifying the shedding of allergy-related molecules only under pro-inflammatory conditions. In this respect, ADAM10 is not significantly upregulated in its expression by neither LPS nor TNF-α[26]. Based on the observed shedding of CD23 from the cell surface, a fluorogenic substrate containing the exact CD23 cleavage sequence Dabcyl-His-Gly-Asp-Gln-Met-Ala-Gln-Lys-Ser-Lys (5-Fam)-NH2) could be designed to detect ADAM8 activity in *in vitro* assays.

Due to this activity towards CD23, it can be postulated that soluble ADAM8 could cleave CD23 from the cell surface *in trans*, i.e. on the adjacent cell. A large amount of recombinant soluble ADAM8 would allow to address this question.

1.3 Fibronectin (FN)

Another described substrate of ADAM8 is Fibronectin (FN). FN is a high-molecular weight (~440kDa) glycoprotein of the extracellular matrix (ECM) that binds to membrane-spanning receptor proteins called integrins[27]. Similar to integrins, FN binds extracellular matrix components such as collagen, fibrin, and heparan sulfate proteoglycans. FN exists as a protein dimer, consisting of two nearly identical monomers linked by a pair of disulfide bonds[27]. The FN protein is produced from a single gene, but alternative splicing of its pre-mRNA leads to several isoforms.

FN plays a major role in cell adhesion, growth, migration, and differentiation, and it is important for processes such as wound healing and embryonic development[27]. Altered FN expression, degradation, and organisation are associated with a number of pathologies, including cancer and fibrosis[28].

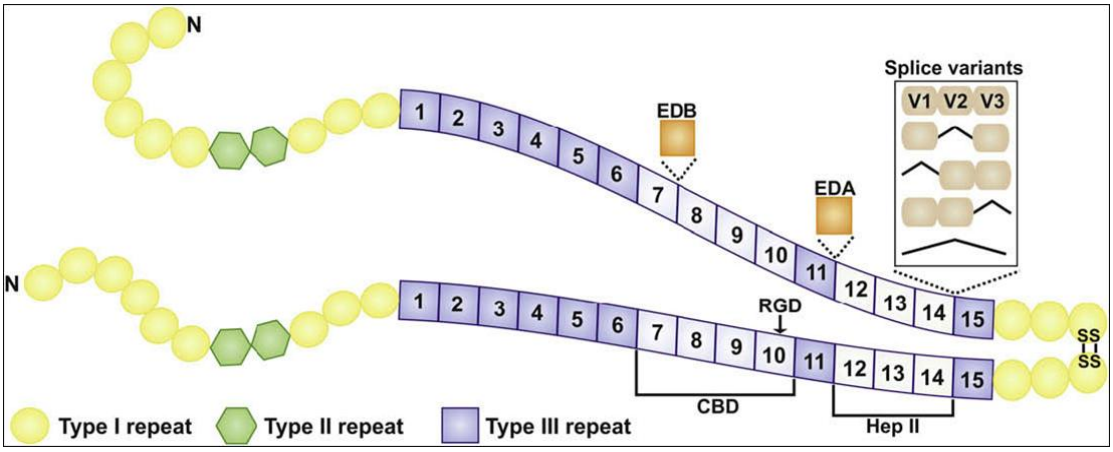

Figure 3: Diagram of dimeric fibronectin

The disulfide bonded nearly identical polypeptide chains consist of homologous type I (circles), II (hexagons), and III (squares) repeats. The RGD containing cell binding domain (CBD) and the HepII domain are indicated by shaded squares. Alternatively spliced exons (EDA, EDB, and V) contribute to the various isoforms of fibronectin. Exon subdivision of the V exon is indicated in the box[29].

Besides shedding of membrane proteins, ADAM8 cleaves molecules of the ECM. As reported for experimental autoimmune arthritis (EAA), a condition associated with enhanced cleavage of ECM molecules, ADAM8 inactivation by introducing the E330Q mutant into an ADAM8 deficient background in mice resulted in a milder disease progression of EAA[30], later shown to be associated with reduced cleavage of FN at the Ala271 redidue[31]. A recent study has identified FN fragments of 25- to 29-kDa in degenerative human intevertebral discs (IVD)[32], and data supporting a pathophysiological role of FN-fragments are emerging: the 29-kDa N-terminal FN-fragment is capable of causing disc degeneration in rabbits[33]. ADAM8 was identified in degenerative IVD tissues and could play an important role in FN fragmentation associated with disc tissue degeneration[32].

In the present study, we will investigate cleavage of FN *in vitro* using recombinant hEctoA8 and FN together for 48 h in 37^{o}C water bath and analyse recombinant hEctoA8 cleavage of FN on tumor cell adhesion and signal transduction.

1.4 Inhibitor of ADAM8

Batimastat, BB-94 (molecular formula: C23H31N3O4S2) is a well-known synthetic inhibitor of metalloproteases containing a peptide domain mimicking the cleavage site of collagen and a hydroxamate group, which is bound by metalloproteases and blocks the zinc ion in the catalytic site of the metalloprotease, respectively. The metalloprotease is thereby inactivated. Since the majority of MPs share a homologous catalytic domain, BB-94 exhibits a broad-spectrum inhibition property[34].

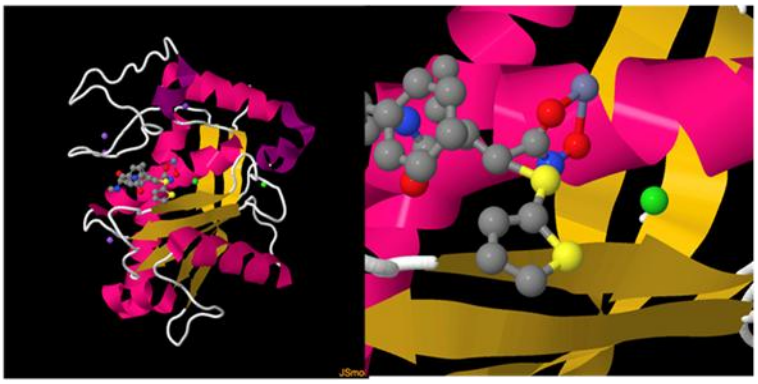

Figure 4: X-ray structure of the ADAM8 MP domain in complex with hydroxamate inhibitor BB-94.
Left: Secondary structure model with BB-94 shown in the catalytic site. Right: Detailed view of BB-94 complexing the Zn ion in the catalytic center by two oxygens (red) from BB-94.

In our study, we would use BB-94 to inhibit catalytic activity of recombinant hEctoA8 and investigate the change of its biological properties; we also would pursue to identify novel and more specific inhibitors by comparing their potency to BB-94.

2. Aims of this study

- Expression and purification of recombinant hEctoA8 protein from supernatants of transfected HEK cells;
- Analysis of cleavage properties of recombinant hEctoA8 with substrates CD23 *in trans* and FN *in vitro*;
- Effect of recombinant hEctoA8 cleavage of FN on tumor cell adhesion and intracellular signaling.

3. Materials

3.1 Cell lines

A stable HEK cell line expressing recombinant hEctoA8 and a CD23 stably transfected Panc1 cell lines were generated by Uwe Schlomann; Pancreatic tumor (Panc1_WT) cells were obtained from Sigma UK; In addition, an ADAM8 overexpressing Panc1 cell line (Panc1_A8) was also generated by Uwe Schlomann as described[12].

3.2 Media and solutions for cell culture

HEK-293 cells and Panc1 cells were cultured in DMEM (Dulbecco's Modified Eagle Medium) High Glucose (4.5 g/l) supplemented with 1% L-Glutamine (200 mM), 1% Penicillin/ Streptomycin 100×, 1 mM sodium pyruvate solution, 1% MEM Non Essential Amino Acids 100× and 10% Fetal Bovine Serum (heat inactivated).

For purification of recombinant hEctoA8 from supernatant, complete growth medium was exchanged by DMEM High Glucose (4.5 g/l) without serum and phenol red on the days before collecting the supernatant and harvesting the cells.

All materials above were bought from PAA Laboratories GmbH.

3.3 Kits

Description	Manufacturer
HisTALON™ Buffer Set	Clontech TAKARA BIOTECHNOLOGY(DALAN)CO.LTD
Pierce® Silver Stain Kit	Thermo Scientific Rockford USA
4%-20% Precast Gel	Expedeon San Diego USA
Mini-PROTEAN®TGX™ Precast Gels*	BIO-RAD USA
WesternBright Chemilumineszenz Substrat Sirius	Biozym Scientific GmbH
SuperSignal® West Femto Maximum Sensitivity Substrate	Thermo scientific, USA

*****The new Mini-PROTEAN and Criterion TGX (Tris-Glycine eXtended) Stain-Free precast gels for PAGE are based on the long-shelf life TGX formation and include unique trihalo compounds that allow rapid fluorescent detection of proteins with stain-free enabled imagers (for example, Chemiluminescence and Fluorescence Instruments (60-FU-SOLO) in our Lab.). The trihalo compounds react with tryptophan residues in a UV-induced reaction to produce fluorescence, which is easily detected by stain-free enabled imagers within gels.

3.4 Antibodies

Antibody	Dilution	Manufacturer
First antibodies		
Anti-ADAM8 (goat polyclonal lgG)	1:2000	Santa Cruz Biotechnology
Anti-CD23(rat monoclonal)	1:100	Roche Diagnostics
Anti-integrin α5 rabbit Ab	1:1000	Cell Signaling Technology
Anti-integrin β1 rabbit Ab	1:1000	Cell Signaling Technology
Anti-p-Akt rabbit Ab	1:1000	Cell Signaling Technology
Anti-p-ERK1/2 Ab	1:2000	Cell Signaling Technology
Anti-β-Tubulin (H-235) rabbit polyclonal	1:500	Santa Cruz Biotechnology
Secondary antibodies		
Anti-goat IgG, HRP-conjugated	1:2000	R&D systems
Anti-rat lgG, HRP-linked	1:2000	Cell Signaling Technology
Anti-rabbit IgG, HRP-linked	1:2000	Cell Signaling Technology
Dnk pAb to Rb IgG(HRP)	1:4000	Abcam®

3.5 Protein ladder

PageRuler™ Plus Prestained Protein ladder is manufactured by Pierce Biotechnology, Thermo Scientific, USA.

3.6 Buffers and Solutions

Buffer and Solutions	Ingredients
Equilibration buffer	50 mM Tris, 150 mM NaCl
5 ×loading buffer	3.125 ml 1 M Tris PH 6.8, 1 g SDS, 4.5 ml Glycerol, 125 µl 1% BPB, 1.25 ml β-Mercaptoethanol
RIPA buffer	50 mM HEPES PH 7.4, 150 mM NaCl, 1% NP-40, 0.5% Sodium Deoxycholate, 0.1% SDS+1 ×complete protease inhibitor, 1 ×Phosstop
10 ×Running buffer	144 g Glycine, 30 g Tris Base, 10 g SDS to 1 L with ddH_2O
10 ×Transfer buffer	144 g Glycine, 30 g Tris Base to1 L with ddH_2O
1 ×Transfer buffer (Western Blot)	100 ml 10 ×Transfer buffer, 200 ml Methanol to 1L with ddH_2O
5% Milk blocking solution	5 g no-fat dry milk powder, 100 µl Tween 20, 100 ml PBS (1 ×)
Substrate assay buffer	1 ml 1 M Tris PH 8.0, 500 µl 1 M $CaCl_2$, 50 µl 1 mM $ZnCl_2$, 1 µl Brij® 35 solution to 50 ml with ddH_2O

3.7 Inhibitor (CT1746)

CT1746(N1-[2-(S)-(3,3-dimethylbutanamidyl)]-N4-hydroxy-2-(R)-[3-(4-chlorophenyl)-propyl] succinamide; Ref.15; obtained from CellTech, now UCB) has Kis against human gelatinase A, gelatinase B, stromelysin 1, collagenase, and matrilysin of 0.04, 0.17, 10.9, 122, and 136 nM, respectively (Kis performed by Jimi P. O'Connell, Cell tech Therapeutics Ltd.). It has negligible activity (>40 µM) against other classes of metalloproteinase such as neprilysin (EC 24. 11), meprin, peptidyl dipeptidase A (ACE), and aminopeptidase N, and, at a concentration of 1 mM, has no apparent cytotoxicity[35].

4. Methods

4.1 Cloning of human ectodomain ADAM8 (hEctoA8) constructs

C-terminally 6×His tagged hEctoA8 constructs were generated by PCR using cloning primers (hA8SgfI 5'-GAGGCGATCGCCATGCGCGGCCTCGGGCTC-3', hA8MluI 5'-GCGACGCGTGGGTGCTGTGGGAGCTCC-3') and ligated into the pCMV6 expression vector (Origene) using the *MluI* and *SgfI* restriction sites, respectively.

4.2 Generation of HEK-293 expression recombinant hEctoA8 cells

HEK-293 cells were transfected with C-terminally 6×His tagged hEctoA8 constructs (cloned in pTarget) and the pRFP-C-RS vector (Origene) encoding for red fluorescence protein (RFP). Control cells were transfected with RFP vector only. Twenty-four hour after transfection, cells were treated with the Resistant RFP-positive cells were isolated by fluorescence-activated cell sorting (FACS). C-terminally 6× His tagged HEctoA8 expression in single-cells clones was analysed by western blot and quantitative reverse transcription PCR.

4.3 Generation of Panc1 expression CD23 cells

Panc1 cells were transfected with pIRESCD23-HA tagged constructs that was kind gift of Professor Zena Werb (San Francisco, USA) as the same way as generation of HEK-293 expression recombinant hEctoA8 cells.

4.4 Recombinant hEctoA8 transfected HEK cell culture

Recombinant hEctoA8 transfected HEK cells were cultivated in 15 ml growth medium (containing 10% heat-inactivated fetal bovine serum, 1% non essential amino acids, 1% sodium pyruvate, 1% streptomycin, 1% Zell Shield^{TM} (the anti

contamination additive for cell cultures, Minerva Biolabs GmbH) and 2% G418) in 75 cm^2 flask. The cells were confluent in 75 cm^2 flask and then were divided into four 175 cm^2 flasks in 20 ml growth medium. The serum free medium 20 ml without phenol red was exchanged to the flask when the cells were confluent; the cells were incubated for 5 days and supernatant were collected and centrifuged at 4,000 rpm for 10 min to eliminate cell debris. Fresh supernatants were used directly for purification or stored at -80^oC.

4.5 Recombinant hEctoA8 purification

TALON Resin was thoroughly re-suspended and equilibrated; the supernatant collected previously was added to the resin and the mixture was gently agitated on a platform shaker to allow his-tagged protein to bind the resin at 4^oC for 1-2 h; then the mixture was centrifuged at 700× g for 5 min and as much supernatant as possible without disturbing the resin pellet was removed carefully; the resin pellet was wash by Equilibration Buffer thoroughly; one bed volume of Equilibration Buffer was added to the resin and re-suspended by vortexing, the resin was transfered to a 2 ml gravity-flow column with an end-cap in place, and the resin was allow to settle out of suspension, the end-cap was removed and the buffer was allowed to drain until it reached the top of the resin bed, making sure no air bubbles were trapped in the resin bed; the his-tagged proteins were eluted by adding 5 bed volumes of Elution Buffer to the column and the eluate was desalted by PD-10 Desalting column with equilibration buffer and collected in 500 μl fractions; the concentration of recombinant hEctoA8 in eluate was measured with NanoDrop-1000 (peQLab). As shown by Fig.5.

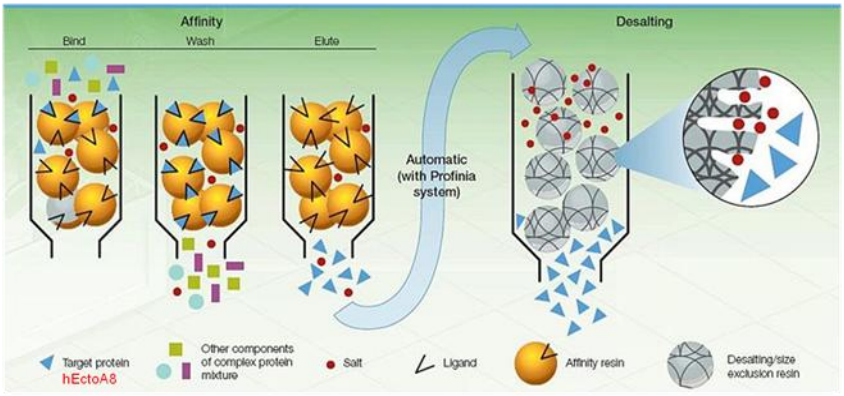

Figure 5: Schematic diagram of TALON affinity chromatography

4.6 SDS-Polyacrylamide gel electrophoresis (SDS-PAGE)

Gel	Ingredient
Stacking gel	30% Acrylamide 0.333 ml 1M Tris PH 6.8 0.25 ml ddH_2O 1.385 ml 10% SDS 20 µl 10% APS 20 µl TEMED 2 µl
Separating gel	30% Acylamide 1.667 ml 1M Tris PH 8.8 1.875 ml ddH_2O 1.364 ml 10% SDS 50 µl 10% APS 40 µl TEMED 4 µl

4.7 Silver Staining

The recombinant hEctoA8 protein purified by TALON affinity was separated via 10% SDS-PAGE gel electrophoresis. Then the gel was washed in ultrapure water for 5 min (×2) and fixed in 30% ethanol: 10% acetic acid solution (i.e., 6:3:1 water: ethanol: acetic acid) for 15 min (×2). Subsequently, the gel was washed in 10% ethanol

solution for 5 min (×2) and incubated in Sensitizer Working Solution for exactly 1 min and washed with two changes of ultrapure water for 1 min each, then the gel was incubated in Stain Working Solution for 30 min. Subsequently, the gel was quickly washed with two changes of ultrapure water for 20 seconds each and developed in Developer Working Solution until the protein bands appeared.

4.8 Protease activity assay

Synthetic fluorescence resonance energy transfer (FRET)-based polypeptide protein substrates have been developed to estimate the protein activity in real-time mode. These substrates are typically composed of a FRET donor and a quencher fluorophore, which are linked by a sequence of amino acid containing a protease cleavage motif. Once the polypeptide is cleaved by the protease, the fluorophore donor separates from the quencher resulting in an increase of fluorescence. Thus, protease activity dynamics can be monitored by tracking the fluorescence changes over time[16] (Fig.6).

PEPDAB013 (Dabcyl-His-Gly-Asp-Gln-Met-Ala-Gln–Lys-Set-Lys (5-FAM)-NH_2) was used as specific substrate for recombinant hEctoA8. The substrate was stored in DMSO at -20^{o}C in a stock solution of 10 mM. After diluting the substrates 1:500 with activity buffer, we added 12.5 µl eluate of recombinant hEctoA8, 37.5 µl activity buffer and 50 µl substrate assay buffer per well in triplicate in a 96-well-plate. For blank wells, 12.5 µl equilibration buffer, 37.5 µl activity buffer and 50 µl substrate assay buffer were added per well. Fluorescence was measured every 2 min with excitation and emission wavelengths of 485 and 530 nm for 180 cycles (6 h), respectively.

For inhibitor of BB-94 and CT-1746, purified recombinant hEctoA8 was incubated with 1nMol of BB-94, CT-1746 (10 µMol, 1 µMol, 100 nMol, 10 nMol and 1 nMol) for 1 h at room temperature (RT) respectively before activity assay.

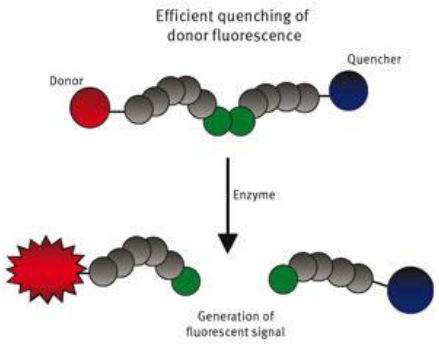

Figure 6: Schematic diagram of polypeptide cleaved by the protease

These substrates are typically composed of a FRET donor and a quencher fluorophore, which are linked by a sequence of amino acid containing a protease cleavage motif. Once the polypeptide is cleaved by the protease, the fluorophore donor separates from the quencher resulting in an increase of fluorescence.

4.9 Purified recombinant hEctoA8 cleaved CD23 from transfected Panc1 cells

Recombinant hCD23 transfected pancreatic cells were grown in DMEM growth medium (containing 10% heat-inactivated fetal bovine serum, 1% non essential amino acids, 1% sodium pyruvate, 1% streptomycin, 1% Zell Shield^{TM} and 2% G418) in 75cm^2 flask. When the cell is confluent in the flask, cell monolayer was detached by 2 ml trypsin/EDTA and cells were diluted to 400/µl, 50 µl cells dilution was planted in 96-well-plate. The serum free medium 50 µl without phenol red was exchanged to the wells as control group, recombinant hEctoA8 1 µg and 2 µg mixed with serum free medium without phenol red (the total volume 50 µl) was exchanged respectively next morning. The supernatant was collected after 1 h, 6 h and overnight for western blot directly or stored in -20^{o}C.

4.10 FN cleavage assay

For recombinant hEctoA8 mediated human FN cleavage, 3 µg, 1.5 µg and 0.75 µg recombinant hEctoA8 were incubated with 3 µg human FN and activity buffer for 48 in 37^{o}C water bath. Recombinant hEctoA8 inhibitor, BB94 1 nMol was added to 3 µg recombinant hEctoA8 with activity buffer and pre-incubated at 37^{o}C for 1h and then add FN incubating for 48 h. Recombinant hEctoA8 3 µg with activity buffer and FN with activity buffer as control groups also incubated in 37^{o}C water bath for 48 h. The

total volume is 60 µl.

After incubation, the mixed solutions were collected and separated using Mini-PROTEAN®TGX™ Precast Gels via electrophoresis and the bands on the gel were shown by rapid fluorescent detection of proteins with stain-free enabled imagers, then the bands were isolated from the gel and send to Dr. Oliver Schilling (Freiburg University) for analysis of FN fragments by Mass Spectrometry.

4.11 FN coating procedure

24-well-plate was coated with 200 µl/well of 20 µg/ml FN in PBS and incubated overnight (or longer) in the cold (2–8 ℃). Then the plate was rinsed with PBS after the remaining solution was carefully aspirated. Subsequently, blocking buffer 2–5% BSA in PBS was added to the wells at least 1 h at room temperature or overnight at 2–8 ℃ (200 µl/well). Blocked plates can be stored, as is, in the refrigerator for several weeks or can be decanted and dried and stored for months in a dessicator. Desiccated material should be rehydrated for 15 min with PBS before use.

Caution: The BSA solution needs to be filtered to remove excess non-specific sticking in the assay caused by insoluble BSA clumps (RIA-grade BSA is usually recommended). Unfiltered material may look clear but the filters will clog while passing the BSA so it is recommended to use prefilters on top of the filter bed to increase the amount of material that will pass.

4.12 Adhesion assay

24 well culture plates were coated described as FN coating procedure; wells coated with PBS were used as negative controls. Recombinant hEctoA8 treatments were prepared by diluting recombinant hEctoA8 to various concentrations to a volume of 150 µl/well with activity buffer. BB94 1 nMol was added to recombinant hEctoA8 10 µg with activity buffer and was pre-incubated at RT for 1 h, then all treatment groups were added to the FN coated well for 24 h at 37^{o}C. Panc1_WT and Panc1_A8 were grown to confluence in DMEM media in 75 cm^{2} flasks, respectively, and cells were

washed with PBS for one time and harvested with Trypsin EDTA. Cells were centrifuged and cell pellet was reconstituted in DMEM media. 2×10^5 cells in 150 µl were then seeded on the wells that were pretreated with recombinant hEctoA8 as described above.

Cells were then incubated for 30 min at 37℃ to allow for adhesion. Non-adherent cells were removed by pipetting out the media, followed by washing the wells for 3 times with PBS. Adherent cells were fixed with 4%PFA for 15 min at room temperature (RT), and then incubated with Hoechst (1:1000 in PBS) for 10 min at RT, and washed with PBS for 3 times.

To maximize the area to be examined for the adherent cell quantification, wells were photographed at 3 conserved areas using Leica fluorescence microscope (×50 magnification). Cells were counted by the software ImageJ. Experiments were repeated at least 3 times with 3 triplicates per condition.

4.13 Western Blot

Western blot was used to detect recombinant hEctoA8 purified by Talon affinity chromatography and soluble CD23 fragments cleaved by recombinant hEctoA8 described as previously, expression of integrin α5β1 and activation of so p-ERK1/2 and p-AKT of protein samples described as follows:

24 well culture plates were coated described as FN coating procedure; wells coated with PBS were used as negative controls. Recombinant hEctoA8 treatments were prepared by diluting 10 µg recombinant hEctoA8 to a volume of 150 µl/well with activity buffer. BB94 1 nMol was added to the recombinant hEctoA8 10 µg with activity buffer and was pre-incubated at RT for 1 h. Then, all treatment groups were added to the FN coated well for 24 h at 37 ^{o}C. Panc1 cells were grown to confluence in DMEM media in 75 cm^2 flask, cells were washed with PBS for one time and harvested with Trypsin EDTA. Cells were centrifuged and the cell pellet was reconstituted in DMEM medium. 2×10^5 cells in 150 µl were then seeded on the wells that were pretreated with recombinant hEctoA8 as described above. Cells were then

incubated for 4 h at 37 ℃ to allow for all cells adhesion and cells were lysed in RIPA buffer and stored at -20 ℃ for western blot.

Protein samples were separated via 10% SDS-PAGE gel electrophoresis and electroblotted onto Protran® nitrocellulose membranes (Whatman GmbH). Nonspecific binding sites were blocked by incubating nitrocellulose membrane for 1h in phosphate-buffered saline containing 5% low-fat dry milk. Membranes were incubated overnight at 4 ℃ with primary antibodies (listed in 3.4 antibodies) and for 1 h at room temperature with secondary antibody linked HRP (Horseradish peroxidase) (listed in 3.4 antibodies). Blots on the membrane were developed using WesternBright Chemilumineszenz Substrat Sirius (Biozym Scientific GmbH) according to the manufacture's instruction. Exposing the membrane to a luminescence reader (Intas, Chemostar Imager) provides an image of the proteins bound to the blot. The Western analysis was made in triplicates. The density of specificbands was measured with a computer-assisted imaging analysis systemand normalized against loading controls. Differences were compared using repeated measure one-way ANOVA.

4.14 Statistical analysis

Results were expressed as the mean ± SEM of at least three separate experiments. Results were analyzed by one-way ANOVA followed by the Fisher's Least Significant Difference (LSD) test. Differences with p values of <0.05 were considered significant.

5. Results

5.1 Purification of recombinant hEctoA8 and its activity assay

The protein recombinant hEctoA8 secreted from transfected HEK-293 cells was purified and identified by western blot, purity of recombinant hEctoA8 protein was analysed by silver staining. As shown in Fig 6, purified recombinant hEctoA8 from the supernatant of transfected HEK cells contained two types of protein (molecular mass 100 and 70 kDa).

In the crude supernatant and in purified fractions, catalytic activity of recombinant hEctoA8 was tested using a peptide derived from the cleavage sequence of CD23-PEPDAB013 Dabcyl-His-Gly-Asp-Gln-Met-Ala-Gln-Lys-Ser-Lys (5-Fam)-NH2) by a FRET assay (Fig 7). Within 6 hours of incubation, there was significant cleavage of PEPDAB013 in the recombinant hEctoA8 fractions. As control, no cleavage was observed in a recombinant human ADAM8 protein consisting of only the disintegrin, cysteine-rich and EGF-like domain of ADAM8 (rhDCEA8).

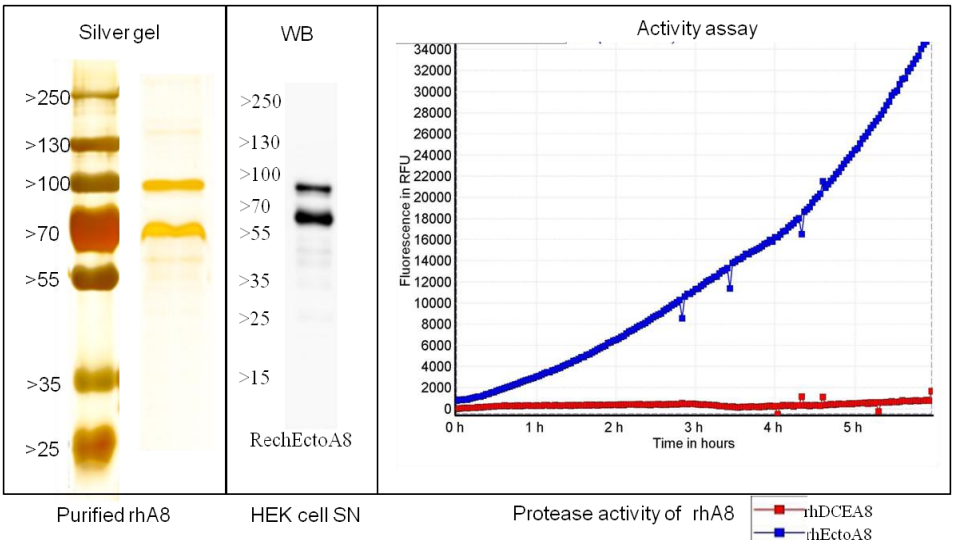

Figure 7: Purification of recombinant hEctoA8 and its proteolytic activity.

Purification of recombinant hEctoA8 from transfected HEK cells analysed by western blot, silver stain, and fluorescence determination of recombinant hEctoA8 activity using substrate PEPDAB013; relative fluorescence intensities increased with incubation time prolonging in PEPDAB013 mixed with recombinant hEctoA8 in the presence of activity buffer (blue line), compared to purified rhDCEA8 domain which has no proteolytic activity (red line).

5.2 The effect of BB-94 (Batimastat) and CT1746 on activity of recombinant hEctoA8

We next tested if a synthetic inhibitor CT1746 is able to block activity of recombinant hEctoA8 and compared its blocking ability to the broad range metalloproteinase inhibitor BB94 known to inhibit ADAM8[3]. Purified recombinant hEctoA8 was incubated with 1nMol of BB-94 and CT-1746 (10 µMol, 1 µMol, 100 nMol, 10 nMol and 1 nMol) for 1 h respectively before the activity assay. In these assays, BB-94 1nMol resulted in completely blocking the activity of recombinant hEctoA8, CT-1746 10 µMol resulted in partially blocking the activity of recombinant hEctoA8. Thus CT-1746 has no inhibitory effect on recombinant hEctoA8 activity in the lower micromolar range (Fig.8).

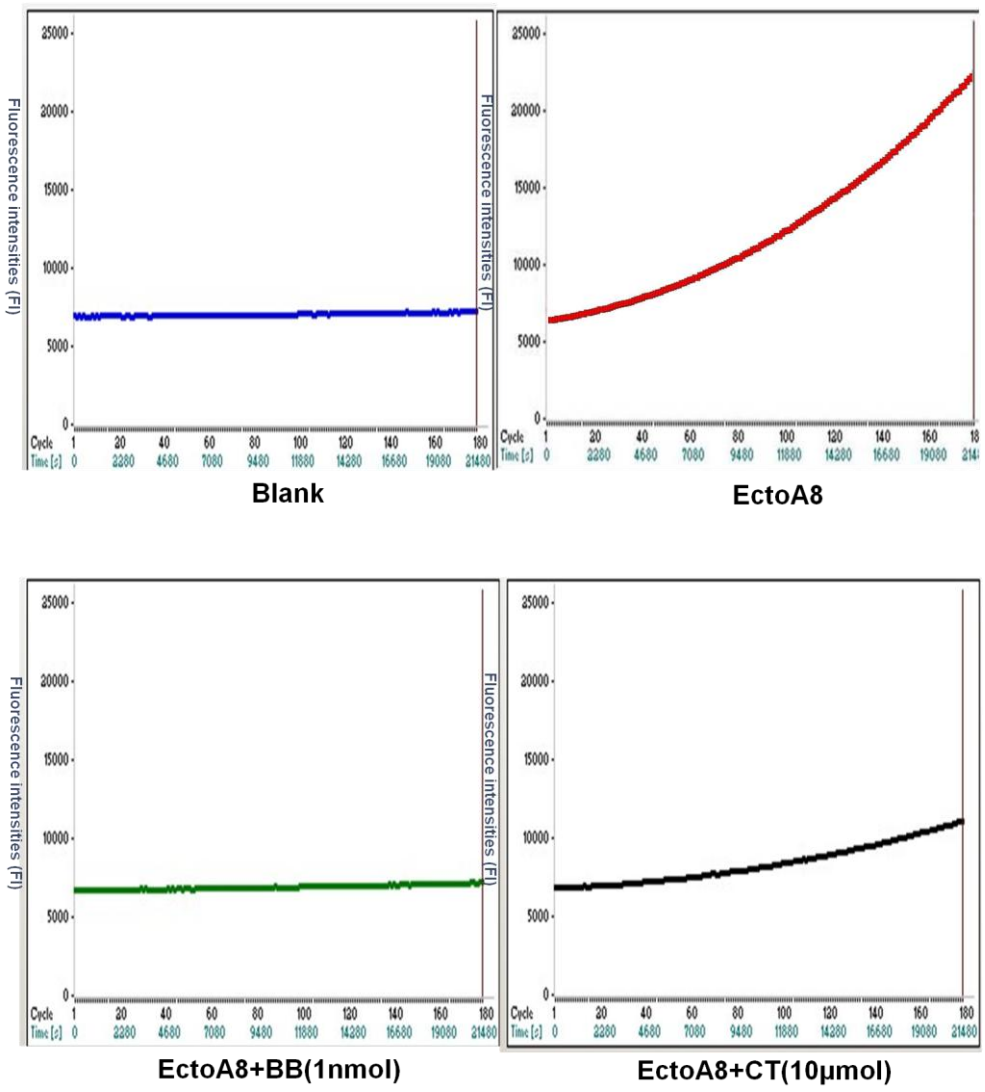

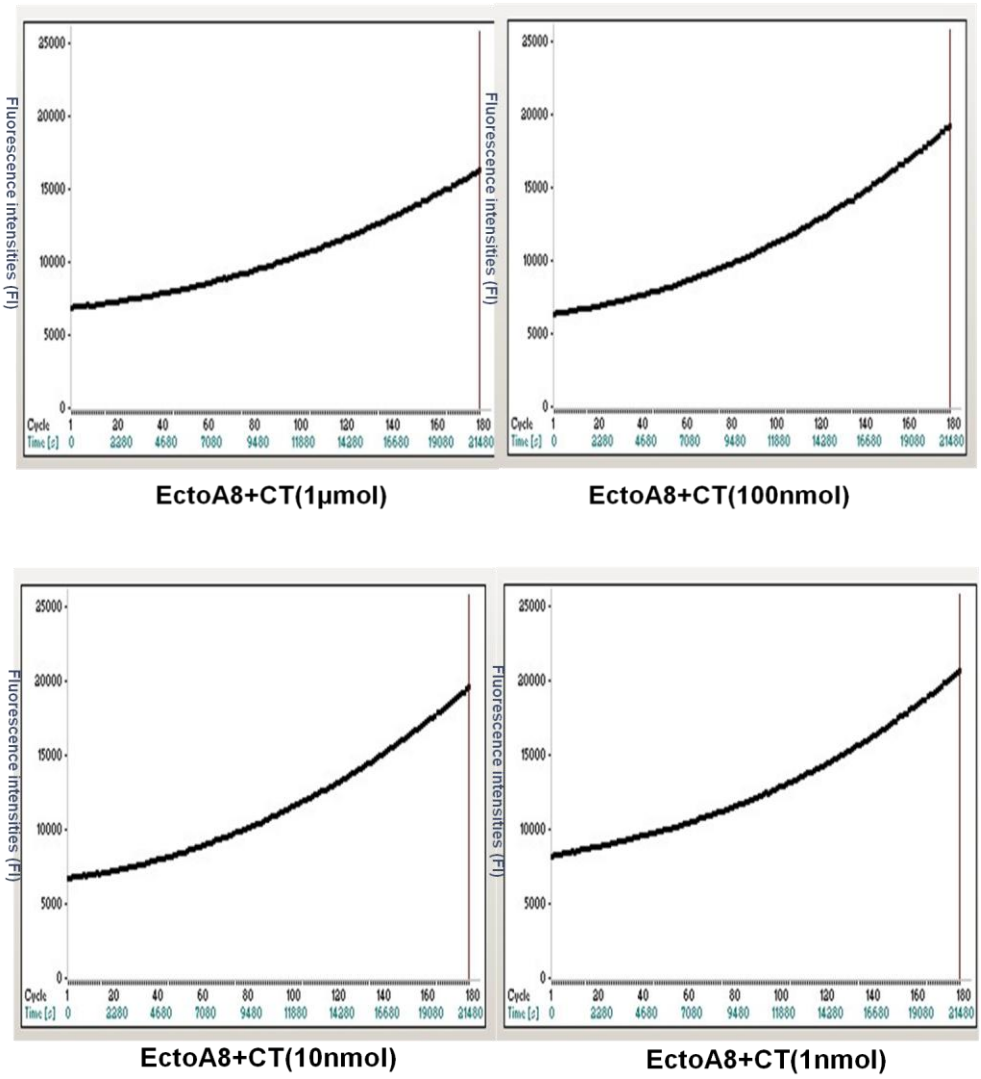

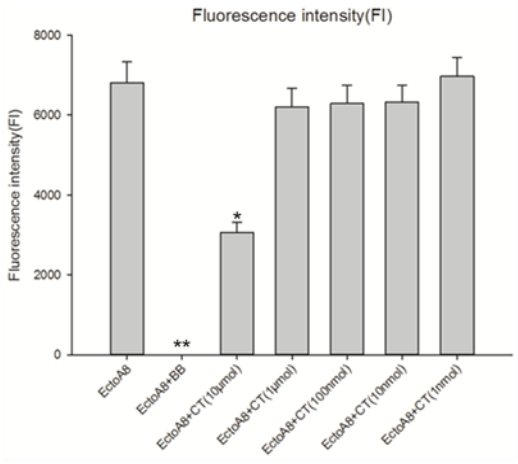

Figure 8: The effect of BB-94 and CT-1746 on activity of recombinant hEctoA8

Effect of treatment with BB-94 and different concentration of CT-1746 on relative fluorescence intensities (FI) of recombinant hEctoA8 cleavage sequence of PEPDAB013, BB94 (1 nMol) resulted in completely blocking activity of recombinant hEctoA8 (**=p<0.01 vs. EctoA8 group); CT1746 10 µMol resulted in partially blocking activity of recombinant hEctoA8 (*=p<0.05 vs. EctoA8 group); no difference was found in other groups.

5.3 Cleavage of CD23 protein from transfected Panc1 cells by recombinant hEctoA8

To test if recombinant hEctoA8 can be used to cleave a substrate *in trans*, Panc1 cells were transfected with CD23 cDNA, after the generation of stable lines by selection with G418, recombinant hEctoA8 1 μg and 2 μg were incubated with CD23 transfected Panc1 cells in phenol red-free medium, the supernatant was collected after 1 h, 6 h and overnight for western blot.

In our study, we found that the CD23 cleaved by recombinant hEctoA8 from Panc1 cell surface yielded soluble CD23 (sCD23) proteins of 37, 33, 25 and 16 kDa. Compared to control group, CD23 transfected Panc1 cells incubated with recombinant hEctoA8, more sCD23 could be detected in the medium in recombinant hEctoA8 1 μg and 2 μg groups at the time point of 1 h ($p<0.05$); the sCD23 proteins of 25 and 16 kDa were more detected at the time point of 6 h compared to control group ($p<0.05$); no difference was found at the time point of overnight for different groups. Compared to recombinant hEctoA8 1μg group, the sCD23 proteins of 37, 33 and 25kDa were more detected at the time point of 1 h in recombinant hEctoA8 2 μg group ($p<0.05$) (Fig.9).

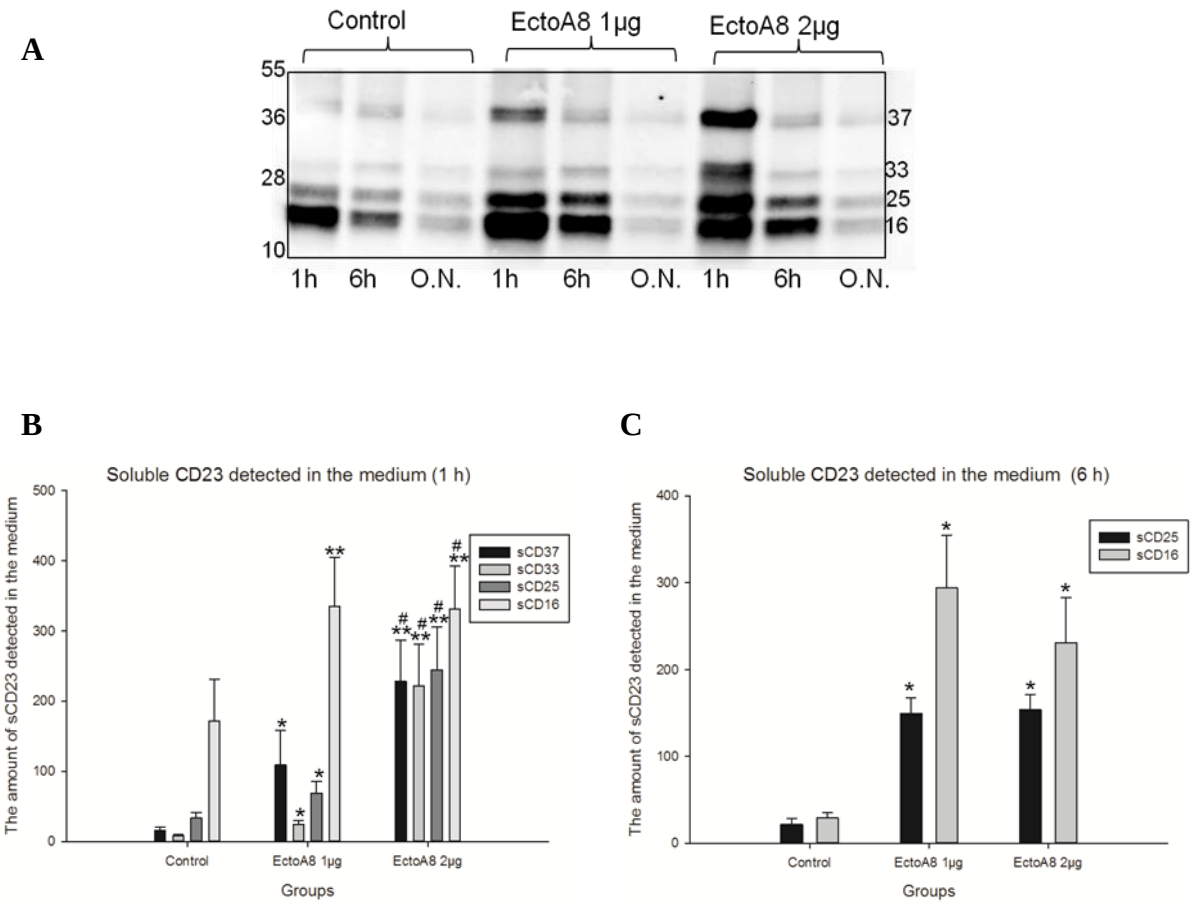

Figure 9: Cleavage of protein CD23 by different dosages of recombinant hEctoA8 from transfected Panc1 cells analysed by western blot at different time points

A: Release of sCD23 by proteolytically active recombinant hEctoA8 from Panc1 stably transfected with CD23 cDNA. Cells were incubated with recombinant hEctoA8 for 1 h, 6 h and overnight, respectively, and the supernatants were analysed by SDS-PAGE, transferred to nitrocellulose membrane, and analysed by Western blot for the presence of sCD23 in the medium. B: Compared to control group, CD23 transfected Panc1 cells incubated with recombinant hEctoA8, more soluble CD23 was detected in the medium after incubation with recombinant hEctoA8 (1 µg and 2 µg) at time point 1 h (*=p<0.05 vs. control group, **=p<0.01vs. control group). Compared to recombinant hEctoA8 1 µg group, the sCD23 proteins of 37, 33 and 25 kDa were more detected in recombinant hEctoA8 2 µg group at time point 1 h (#=p<0.05 vs. EctoA8 1 µg group). C: The sCD23 proteins of 25 and 16 kDa were increased at time point 6 h compared to control group (*=p<0.05 vs. control group). The Western blot analysis was made in triplicates.

5.4 FN cleaved by recombinant hEctoA8 *in vitro*

Soluble recombinant hEctoA8 was isolated and purified from supernatants of transfected HEK cells according to the protocol, the protein preparations were used in different amounts for cleavage assays with FN as a substrate (Fig.10). Purified recombinant hEctoA8 and FN served as controls. When recombinant hEctoA8 was incubated with FN, cleavage resulted in 9 fragments of different molecular weights. As additional control, metalloproteinase inhibitor BB94 was used to inhibit recombinant hEctoA8 proteolytic activity. BB94 (1 nMol) completely inhibited recombinant hEctoA8 activity.

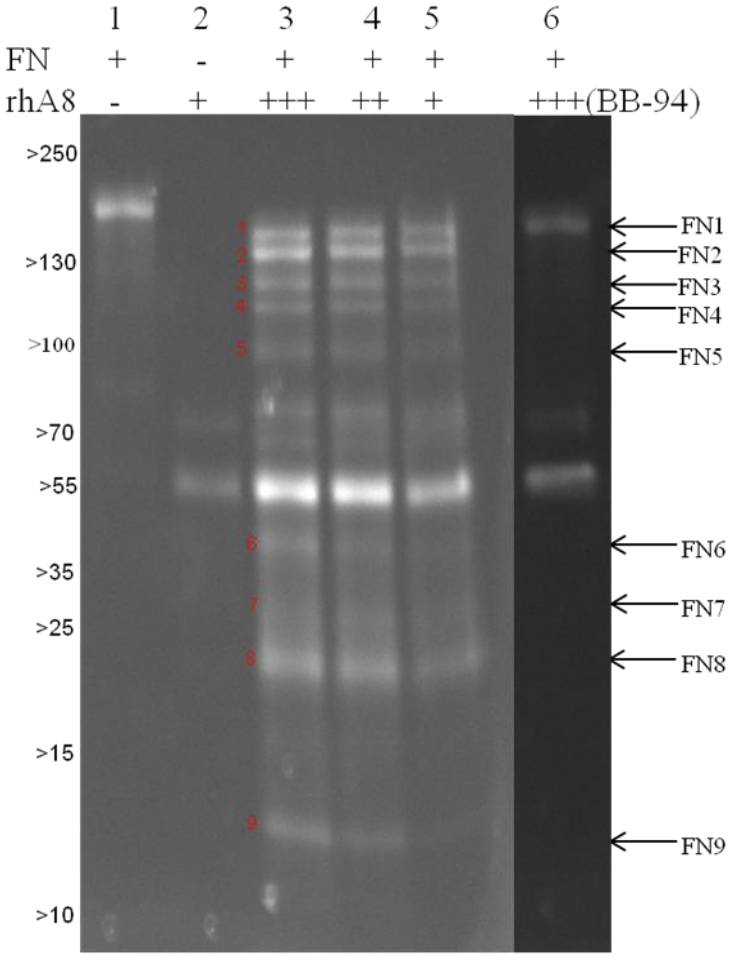

Figure 10: FN cleaved by recombinant hEctoA8 *in vivo*

Purified recombinant hEctoA8 proteases tested with FN. The bands were separated using Stain-Free precast gels and shown by stain-free enabled imagers. The 1st lane shows FN alone and the 2st lane shows recombinant hEctoA8 alone, the 3st lane to 5th lane showed that 3 µg (+++), 1.5 µg (++) and 0.75 µg (+) recombinant hEctoA8 was incubated 3 µg (+) FN for 24 h at 37 °C, the 6th lane showed that the cleavage reaction of 3 µg (+) FN with 3 µg (+++) recombinant hEctoA8 was performed in the presence of BB94 (1 nMol).

5.5 MS analysis of FN fragments cleaved by recombinant hEctoA8

The fragments of FN detailed from recombinant hEctoA8 cleavage (Fig.10) were isolated from the gel, digested with sequence/grade trypsin and the resulting peptide fragements were subsequently analysed by Mass Spectrometry (Fig.11) (see appendix9.1):

A

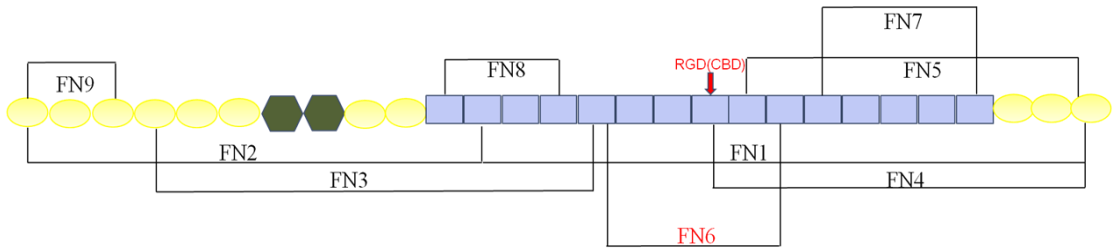

B

Fragment	Position(AA~AA)	Predicted MW(kDa)
FN1	RGQPRQ~REDSRE (1035-2386)	169
FN2	MLRGPG~TVGLTR(0-1035)	129
FN3	AAVYQP~VKDDKE(291-1252)	119
FN4	PGSK ST~REDSRE(1506-2386)	110
FN5	TDVDVD~REDSRE(1656-2386)	91
FN6	RVTWAP~PVTGYR(1285-1575)	38
FN7	TGYIIK~GATYNV(1940-2180)	31
FN8	YAVEEN~TKLDAP(881-1073)	22.4
FN9	MLRGPG~ TYERPK(0-109)	12

Figure 11: MS analysis of FN fragments cleaved by recombinant hEctoA8

A: Schematic representation of FN fragments cleaved by recombinant hEctoA8. B: Fragment sequences analysed by Mass Spectrometry and predicted molecular weights (MW) shown in the table.

5.6 Recombinant hEctoA8-mediated cleavage of FN reduced human pancreatic cells adhesion

To further explore if recombinant hEctoA8-mediated cleavage of FN affect tumor cell adhesion, FN coated wells were treated with increasing concentration of recombinant hEctoA8 at 37℃ for 24 h. 2×10^5 cells in 150 µl were then seeded in the wells that were pretreated with recombinant hEctoA8 as described above. Recombinant hEctoA8 treatment resulted in a dose-dependent decrease in pancreatic cells adherence to FN-coated wells. This decrease reached significance ($p<0.05$) when

recombinant hEctoA8 was used in amounts of 1 µg, 5 µg and 10 µg. Pre-incubation of 10 µg recombinant hEctoA8 with 1 nMol of BB94 restored pancreatic cells adhesion to FN-coated wells (p<0.05), while treating the wells with BB94 alone showed no difference in cell adhesion compared to FN-coated wells (p>0.05). Non-specific adherence of cells to the wells was negligible in the experimental condition as only low number of cells adhered to wells that were coated with PBS in the control group. Compared to the Panc1_WT cell line, more Panc1_A8 cells attached to the coated plate with high significance (p<0.01) (Fig.12, Fig.13, Fig.14).

A

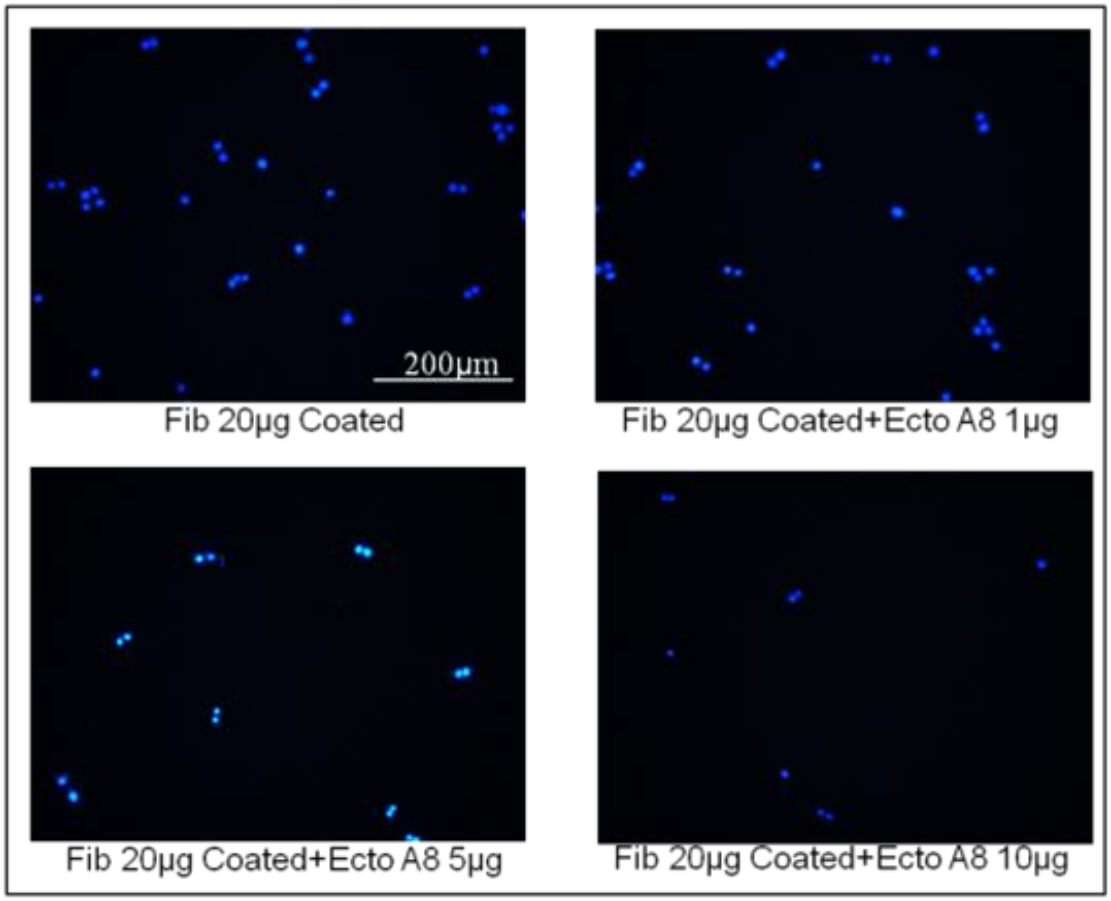

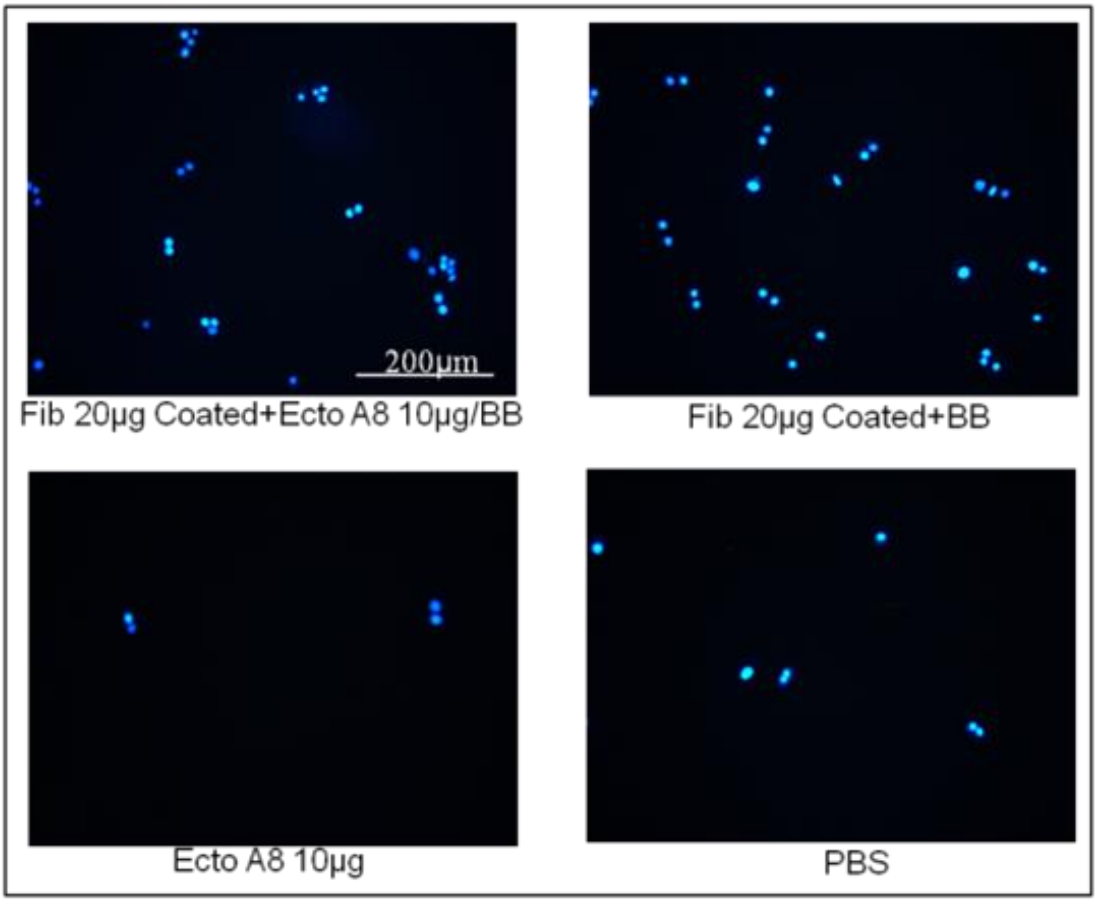

B

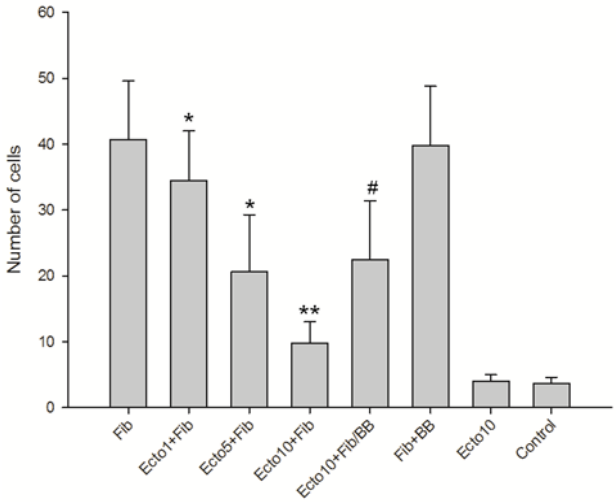

Figure 12: Adhesion assay with Panc1_WT cells

A: Representative images (50×) of adherent Panc1_WT cells on FN-coated (20 µg/ml) wells pre-treated with increasing concentrations of recombinant hEctoA8 with or without BB94 (inhibitor) (1nMol) and with BB94 alone. **B:** Quantification of adherent cells. Results are presented as mean ±SEM of n=3 with three triplicates per condition (*= p<0.05 vs. Fib group, **=p<0.01 vs. Fib group, #=p<0.05 vs. Ecto10+Fib group). Pre-coated wells with PBS were used as negative control.

A

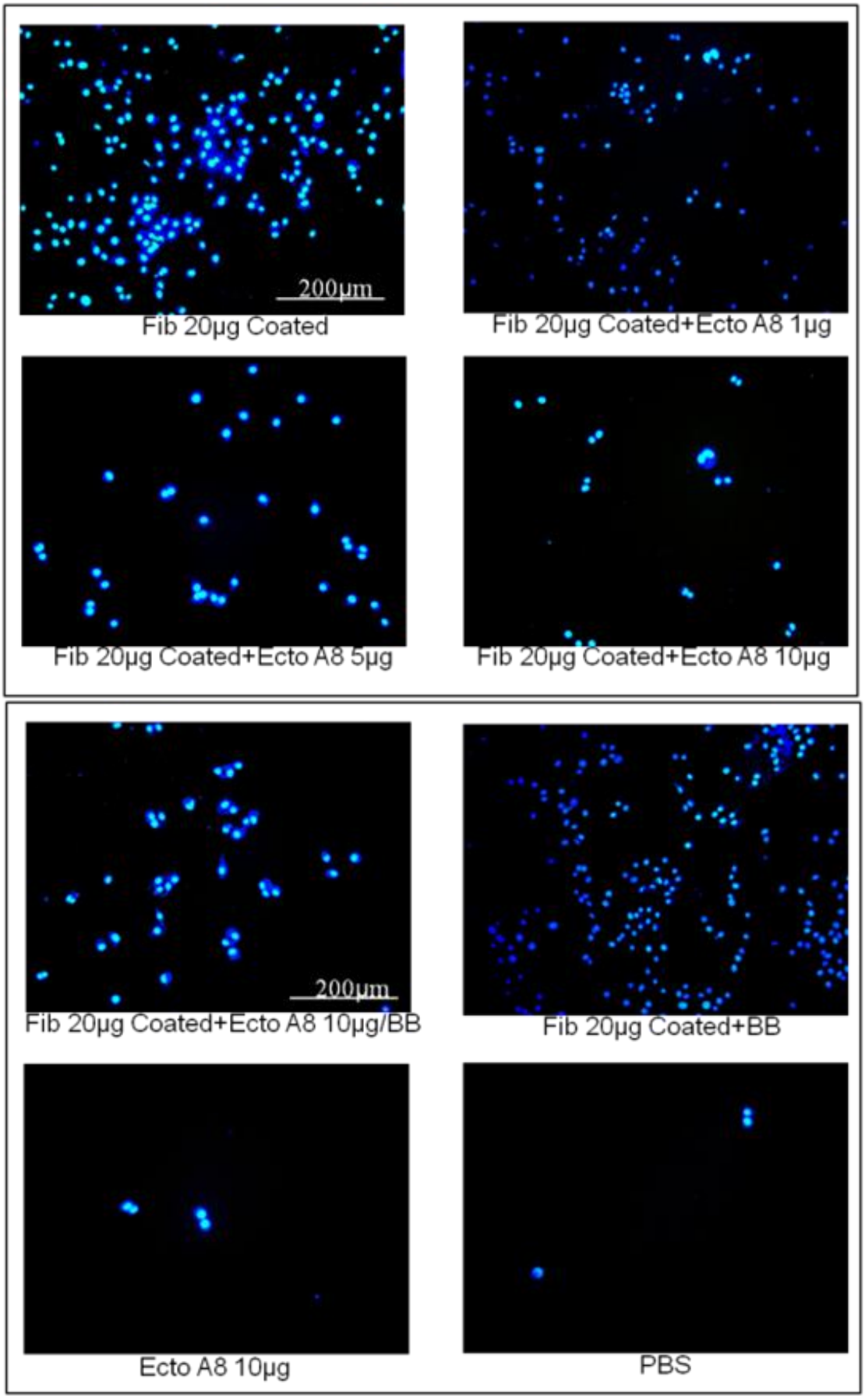
200μm
Fib 20μg Coated
Fib 20μg Coated+Ecto A8 1μg
Fib 20μg Coated+Ecto A8 5μg
Fib 20μg Coated+Ecto A8 10μg
200μm
Fib 20μg Coated+Ecto A8 10μg/BB
Fib 20μg Coated+BB
Ecto A8 10μg
PBS

B

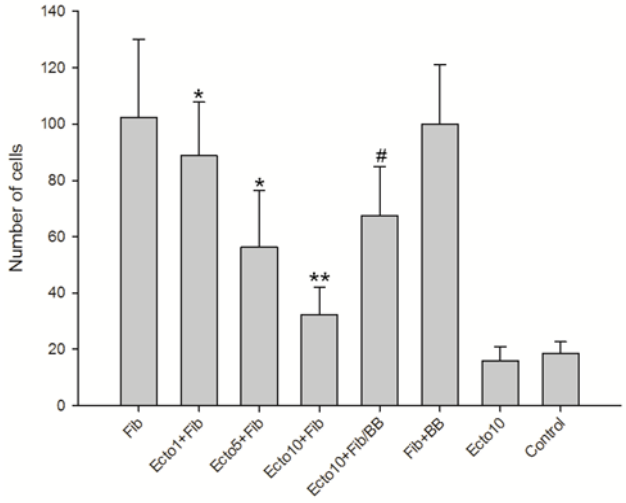

Figure 13: Adhesion assay with Panc1_A8 cells

A: Representative images (50×) of adherent Panc1_A8 cells on FN-coated (20 µg/ml) wells pre-treated with increasing concentrations of recombinant hEctoA8 with or without BB94 (inhibitor) (1 nMol) and with BB94 alone. B: Quantification of adherent cells. Results are presented as mean ±SEM of n=3 with three triplicates per condition (*=p<0.05 vs. Fib group, **=p<0.01 vs. Fib group, #=p<0.05 vs. rhEcto10+Fib group). Pre-coated wells with PBS were used as negative control.

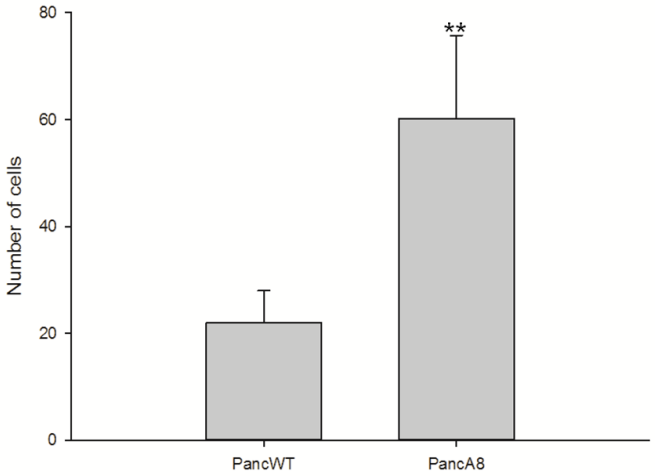

Figure 14: Quantification of cells adhesion for Panc1_ WT cells vs. Panc1_A8 cells

Adhesion of Panc1_ WT cells vs. Panc1_A8 cells, the number of cells was counted by the software ImageJ. Results are presented as mean ±SEM of n=24 with three triplicates per condition. Compared to Panc1_ WT cells, the number of Panc1_A8 cells attached much more (**=p<0.01 vs. Pan_ WT group).

5.7 Effect of FN cleavage on integrin α5 expression

Since the classical fibronectin receptor on the cell membrane is integrin α5β1, we sought to explore whether integrin α5 is involved in recombinant hEctoA8-mediated FN cleavage reducing tumor cells adhesion, so the levels of integrin α5 were analysed in different treatment groups as follows. Panc1 cells expressing integrin α5 weakly was considered as control group; the expression of integrin α5 increased significantly in the presence of FN (p<0.01); when pretreated with recombinant hEctoA8; the expression of integrin α5 was significantly decreased (p<0.05); when pretreated with BB94 for blocking the activity of recombinant hEctoA8, the expression of integrin α5 was partly restored (p<0.05); the activity buffer had no effect on the expression of integrin α5 (Fig.15).

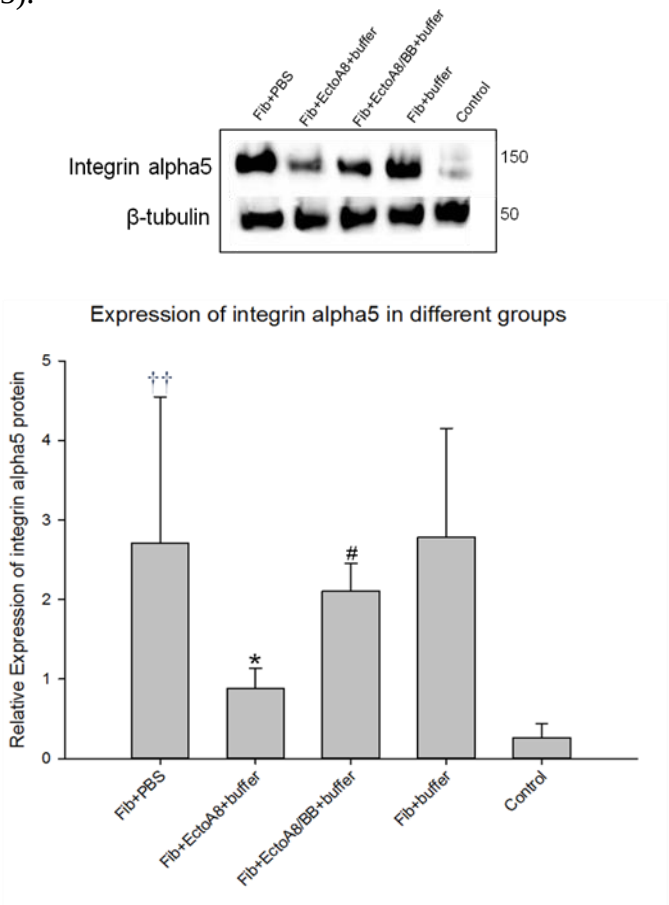

Figure 15: Expression of integrin α5 determined by western blot

In the presence of FN, the expression of integrin α5 was increased significantly (††=p<0.01 vs. control group); Pretreated with recombinant hEctoA8, the expression of integrin α5 decreased (*=p<0.05 vs. Fib group); Pretreated with BB94 to block the activity of recombinant hEctoA8, the expression of integrin α5 was partly restored (#=p<0.05 vs. Fib+EctoA8 group). The Western blot analysis was made in triplicates.

5.8 Effect of FN cleavage on integrin β1 expression

As β-subunit, integrin β1 is part of the FN receptor. Integrin β1 can form heterodimers with the most different alpha-subunits (at least 11), 12 different integrins formed heterodimers with integrin β1 that all bind to ECM protein ligands, namely collagen, laminin, fibronectin, tenascin C and vitronectin[36]. Thus, we explored whether integrin β1 is involved in recombinant hEctoA8-mediated FN cleavage that reduces tumor cells adhesion. Western blot results showed that in contrast to α5 subunit expression, the cellular concentration of integrin β1 is not changed in the reduction of Panc1 cell adhesion caused by ADAM8-dependent cleavage of FN (Fig.16).

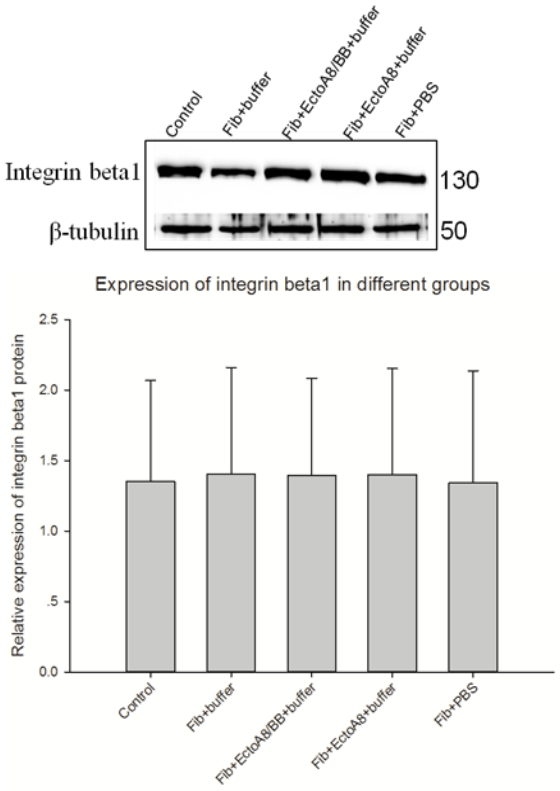

Figure 16: Expression of integrin β1 determined by western blot

Panc1 cells were seeded on FN coated plates as positive control and cells were seeded on PBS coated plates as negative control, cells were then incubated for 4 h 37 ℃ to allow for all cells adhesion and cells were lysed in RIPA buffer for western blot. The expression of integrin β1 showed no difference in different groups. The Western blot analysis was made in triplicates.

5.9 Effect of FN cleavage on activation of p-ERK1/2 and p-Akt

To explore whether recombinant hEctoA8-mediated FN cleavage affects signal transduction in Panc1 cells, expression of activated p-ERK1/2 and p-Akt were analysed in different treatment groups (Fig.17, 18). No significant difference was found; so that we concluded recombinant hEctoA8-mediated FN cleavage does not affect activation of p-ERK1/2 and p-Akt in Panc1 cells.

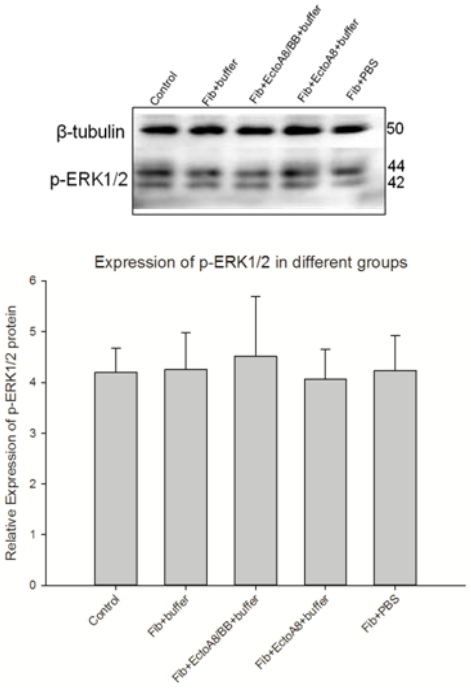

Figure 17: Expression/Activation of p-ERK1/2 determined by western blot

Panc1 cells were seeded on FN coated plates as positive control and cells were seeded on PBS coated plates as negative control, cells were then incubated for 4 h 37 ℃ to allow for all cells adhesion and were lysed in RIPA buffer for western blot. The activation of p-ERK1/2 showed no difference in different groups. The Western blot analysis was made in triplicates.

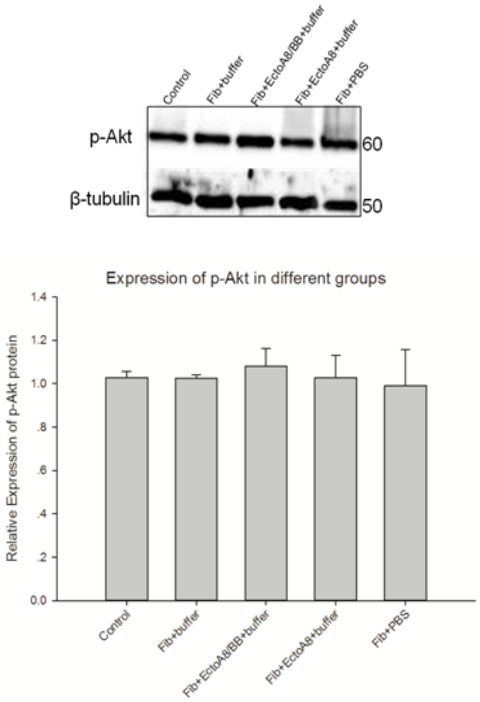

Figure 18: Expression/Activation of p-Akt determined by western blot

Panc1 cells were seeded on FN coated plates as positive control and cells were seeded on PBS coated plates as negative control, cells were then incubated for 4 h 37 ℃ to allow for all cells adhesion and were lysed in RIPA buffer for western blot. The activation of p-Akt showed no difference in different groups. The Western blot analysis was made in triplicates.

6. Discussion

6.1 Purification of recombinant hEctoA8 from transfected HEK cells

In our studies, we successfully purified biologically active recombinant hEctoA8 protein expressed in stably transfected HEK-293 cells. Western blot analysis using goat anti-hA8 antibody confirmed that the recombinant hEctoA8 protein is present in HEK cell supernatants; SDS-PAGE silver staining analysis confirmed the purity obtained using TALON affinity chromatography. The recombinant hEctoA8 purified by TALON affinity yielded protein bands with apparent molecular weights of 100 kDa and 70 kDa which represent the proform and the activated form of recombinant hEctoA8. The theoretical molecular weight for full-length recombinant hEctoA8 is ~92 kDa. The slightly higher apparent molecular weight (100 kDa) for the proform of recombinant hEctoA8 is likely to be due to post-translational modifications, as shown earlier by Schlomann et al.[3]. Removal of the prodomain was shown by Schlomann et al. to result in a molecular form of 72 kDa, so presumably the 70 kDa band we observed represents active recombinant hEctoA8[3].

6.2 Proteolytically active function of recombinant hEctoA8

To investigate recombinant hEctoA8 catalytic activity, a peptide derived from CD23 as a known substrate of ADAM8[16] was used to monitor activity as fluorescence increase. This setup allows for identification of ADAM8 inhibitors. We found that in the absence of inhibitors, recombinant hEctoA8 cleaves the CD23 peptide efficiently, consistent with the previous studies that ADAM8 cleavage was observed at two adjacent amino acid residues (SNQLAQ/K/SQV) for CD23[14]. The hydroxamate-based MMP inhibitor CT1746 (obtained from Cell Tech, now UCB) was tested for inhibition of recombinant hEctoA8 catalytic activity. With different concentrations of CT1746, we only found that CT1746 10 μmol partially blocked the catalytic activity of recombinant hEctoA8. Since efficient hydroxamate inhibitors

inhibit MMPs/ADAMs in a nanomolar range. CT1746 is not an effective inhibitor for recombinant hEctoA8 activity, as compared to BB-94, which has an IC_{50} value of ~50 nM for ADAM8[3].

Given the functionality of the recombinant hEctoA8, we were further interested in analysing the possibility of CD23 shedding by hEctoA8 from CD23 expressing cells. This experimental setup is similar to CD23 release by soluble ADAM8 MP domain released from adjacent cells, i.e. *in trans*. To investigate this, purified recombinant hEctoA8 was incubated with Panc1 cells stably expressing full-length CD23. It was found that CD23 cleaved by recombinant hEctoA8 from Panc1 cells yielded soluble CD23 (sCD23) fragments of 37, 33, 25, and 16 kDa molecular weight. Some of these fragments were reported to be released from the cell surface of cells when ADAM8 was present on the cell membrane, i.e. in *cis*[15]. Our finding is consistent with the results that under physiological conditions, CD23 can be released from the cell surface as a range of diffusible sCD23 proteins which could play an important role for the up-regulation of IgE synthesis by interaction with B cells[25].

CD23, the low affinity IgE receptor, is expressed on B cells, monocytes, macrophages, and eosinophils [37]and is cleaved from the cell surface to generate a number of soluble forms. Both membrane-bound and soluble forms of CD23 have been shown to be elevated in a number of diseases such as asthma, rheumatoid arthritis, and inflammatory bowel disease[24]. Soluble forms of CD23, in addition to their role for the up-regulation of IgE synthesis by interaction with B cells [25], can promote the induction of inflammatory cytokines by macrophages[24]. So membrane-bound as well as soluble ADAM8 involved in shedding and cleaving of CD23 may be the basis of pathophysiology of these diseases.

6.3 FN cleaved by recombinant hEctoA8

Another ADAM8 substrate that was analysed is human plasma FN used in our studies. *In vitro*, recombinant hEctoA8 was incubated with FN, and the cleavage resulted in products with approximate molecular weights of 169, 129, 119, 110, 91, 38, 31, 22.4 and 12 kDa. Of these fragments, the fragment of 38 kDa could be of great interest,

since this fragment contains the RGD motif that is critical for cell adhesion. FN is a core component of many extracellular matrices where it regulates a variety of cell activities through direct interactions with cell surface integrin receptors[38]. FN matrix is important for normal cell adhesion and growth; both decreased expression and elevated degradation of FN have been shown to be responsible for some of the morphological changes observed in tumors and tumor-derived cell lines[38]. As a major protein in blood and a component of the wound provisional matrix, plasma FN contributes to tissue repair and neuronal survival following cerebral ischemia[39]. Clearly, FN is a key component in many ECM-dependent processes *in vivo*. Ruel et al. have identified FN in intervertebral disc (IVD) tissue and found that FN-fragments cleaved by ADAM8 play important role for initiation and progression of disc degeneration, they found 25- and 29-kDa FN-fragments cleaved by ADAM8 existed in the degenerative IVD of surgical tissue[32]. Our finding confirmed that recombinant hEctoA8 with its catalytic function of ADAM8 can cleave FN into 9 different fragments which included 31- and 22.4- kDa fragments that have the similar molecular weight as demonstrated in the previous study[32].

6.4 Effect of recombinant hEctoA8 cleavage of FN on pancreatic cell adhesion and expression of integrin α5β1

Recently published data show that ADAM8 has a critical role in pancreatic cancer progression[12]. To analyse if the observed FN cleavage has physiological consequences such as influencing adhesion/de-adhesion of tumor cells, Panc1_WT and Panc1_A8 cells overexpressing ADAM8 were seeded out on a plastic surface coated with FN either uncleaved or cleaved with hEctoA8. As expected we initially found that recombinant Panc1_ A8 tumor cells attached much better to FN coated surface than Panc1_WT cells due to the interactions between ADAM8 and FN. These results confirmed that ADAM8 itself plays an important role in cell adhesion, consistent with a previous study[3]. Moreover, ADAM8 protease cleaves FN [31] which affects normal cell adhesion and growth[38]. We found that cleavage of FN resulted in reduced tumor cell adhesion. The effect on cell adhesion was partially restored with BB-94 present.

In addition to the previous studies[40], we found here that plasma FN is cleaved by recombinant hEctoA8 in a dose-dependent manner resulting in decreased cell adhesion.

FN regulates a variety of cell activities through direct interactions with cell surface integrin receptors[38], and previous studies demonstrated that the fate of integrin α5 is regulated by matrix-capable FN[41]. In accordance with that we also found that integrin α5 levels decrease within 4 h when FN is cleaved by recombinant hEctoA8. The status of extracellular FN itself could modulate integrin α5 fate via its impact on the binding and activation of other cell-surface receptors[41]. FN in its matrix form is able to engage in multidomain interactions with other cell extracellular components[41]. Some studies found that cells secrete FN as a disulfide-bonded dimer that binds to the integrin α5β1 receptor via the cell-binding domain located in the 10th type 3 repeat of FN[42], but cleavage of FN had no effect on the expression of integrin β1 in our study.

The essential peptide sequence of the initial FN cell binding domain was identified as RGD and subsequently a synergistic sequence PHSRN was identified[43]. Synthetic RGD peptides have been created and have facilitated the identification of integrin cell surface receptors involved in cell attachment. The sequence of FN fragments analysed by Mass Spectrometry showed that the fragment contained RGD peptides cleaved by recombinant hEctoA8 located at the amino acid positions 1285-1575 according to our results. The classic FN receptor is integrin α5β1 and aberrant expression of this receptor has been associated with tumorigenicity[44]. Malignant cell lines are often surrounded by matrix with both increased amounts of FN and integrin α5β1 expression. This integrin participates in the incorporation of FN into matrix and increased metastasis[45]. Integrin α5 levels decreased in 4 h later when FN is cleaved by recombinant hEctoA8 in our study showed that their interaction play an important role in cell adhesion.

There are two explanations for decreased cell adhesion in the cleavage of FN by recombinant hEctoA8. One is that the sequence RGD of FN was cleaved off from the total FN by recombinant hEctoA8; the other explanation could be that the receptor of FN-integrin α5 is not expressed without stimulation by intact FN.

6.5 Effect of recombinant hEctoA8 cleavage of FN on p-ERK1/2 and p-Akt activation of pancreatic cells

ERK1 and ERK2 are 84% identical in sequence and share many if not all functions. For this reason they will be referred to as ERK1/2. ERK1/2, like nearly all protein kinases, contains unique N- and C-terminal extensions that provide signaling specifity[46]. ERK1/2 is a ubiquitous regulator of multiple cellular processes such as proliferation, differentiation, survival, and transformation. Activation of ERK1/2 (p-ERK1/2) can lead to genomic instability and subsequent tumor progression[47].

Akt, also known as protein kinase B, is a serine-threonine kinase that comprises a family of three different protein isoforms: Akt1, Akt2, and Akt3. Akt is a key regulator of PI3K and mTOR signaling, and therefore its activation is an important driver of malignant progression and chemoresistance. Activated Akt can phosphorylate the tumor suppressor protein tuberous sclerosis protein2 (TSC2 or tuberin) to attenuate its negative regulation of PI3K pathway through mTOR inhibition[48]. Activation of Akt has been reported in 28/46 (61%) pancreatic tumor samples[49].

The extracellular matrix (ECM) and cytokines are important mediators of neoplastic cells of tumor development process whose net effects are determined by a complex series of interactions. Extracellular signals can also alter the expression of ECM proteins and cytokines, creating feedback loops that may contribute to tumor development[50]. To explore whether recombinant hEctoA8-mediated FN cleavage is involved in signal transduction in pancreatic tumor cells, we examined the expression of p-ERK1/2 and p-Akt. Our results demonstrated that cleavage of FN by recombinant hEctoA8 has no effect on the activation of p-ERK1/2 and p-Akt.

7. Conclusion

Purified recombinant hEctoA8 containing the catalytic function of ADAM8 can cleave CD23 in cells *in trans* and FN *in vitro*; CD23 cleavage resulted in fragments of 37, 33, 25 and 16 kDa and FN cleavage by recombinant hEctoA8 resulted in 9 fragments, one fragment of 38 kDa contains a RGD motif essential for cell adhesion. Functionally, FN cleavage resulted in reduced tumor cell adhesion and decreased expression of integrin α5; however, cleavage of FN by recombinant hEctoA8 has no effect on the expression of integrin β1, the activation of p-ERK1/2 and p-Akt.

8. REFERENCES

1. Yoshidu S, Setoguchi M, Higuchi Y, Akizuki S, Yamamoto S (1990) Molecular cloning of cDNA encoding MS2 antigen, a novel cell surface antigen strongly expressed in murine monocytic lineage. Int Immunol 2: 585-91.
2. Koller G, Schlomann U, Golfi P, Ferdous T, Naus S, Bartsch JW (2009) ADAM8/MS2/CD156, an emerging drug target in the treatment of inflammatory and invasive pathologies. Curr Pharm.Des 15: 2272-81.
3. Schlomann U, Wildeboer D, Webster A, Antropova O, Zeuschner D, Knight CG, Docherty AJ, Lambert M, Skelton L, Jockusch H, Bartsch JW.The metalloprotease disintegrin ADAM8 (2002) Processing by autocatalysis is required for proteolytic activity and cell adhesion. J Biol Chem 277: 48210-9.
4. Schlomann U, Rathke-Hartlieb S, Yamamoto S, Jockusch H, Bartsch JW (2000) Tumor necrosis factor alpha induces a metalloprotease-disintegrin, ADAM8 (CD 156): implications for neuron-glia interactions during neurodegeneration. J. Neurosci 20: 7964-71.
5. Valkovskaya N, Kayed H, Felix K, Hartmann D, Giese NA, Osinsky SP, Friess H, Kleeff J (2007) ADAM8 expression is associated with increased invasiveness and reduced patient survival in pancreatic cancer. J Cell Mol Med 11: 162-1174.
6. Wildeboer D, Naus S, Amy Sang QX, Bartsch JW, Pagenstecher A (2006) Metalloproteinase disintegrins ADAM8 and ADAM19 are highly regulated in human primary brain tumors and their expression levels and activities are associated with invasiveness. J Neuropathol Exp Neurol 65: 516-527.
7. Ishikawa N, Daigo Y, Yasui W, Inai K, Nishimura H, Tsuchiya E, Kohno N, Nakamura Y (2004) ADAM8 as a novel serological and histochemical marker for lung cancer. Clin Cancer Res10: 8363-8370.
8. Fritzsche FR, Jung M, Xu C, Rabien A, Schicktanz H, Stephan C, Dietel M, Jung K, and Kristiansen G (2006) ADAM8 expression in prostate cancer is associated with parameters of unfavorable prognosis. Virchows Arch 449: 628-636.
9. Zielinski V, Brunner M, Heiduschka G, Schneider S, Seemann R, Erovic B,

Thurnher D (2012) ADAM8 in squamous cell carcinoma of the head and neck: a retrospective study. BMC Cancer12: 76.

10. Zhang R, Yuan Y, Zuo J, Liu W (2012) Prognostic and clinical implication of a disintegrin and metalloprotease8 expression in pediatric medulloblastoma. J Neurol Sci 323: 46-51.
11. Li Z, Liao Q, Wu Y, Liao M, Hao Y, Zhang S, Song S, Li B, Zhang YD (2012) Upregulation of a disintegrin and metalloprotease8 influences tumor metastasis and prognosis in patients with osteosarcoma. Pathol Oncol Res18: 657- 661.
12. Schlomann U, Koller G, Conrad C, Ferdous T, Golfi P, Garcia AM, Höfling S, Parsons M, Costa P, Soper R, Bossard M, Hagemann T, Roshani R, Sewald N, Ketchem RR, Moss ML, Rasmussen FH, Miller MA, Lauffenburger DA, Tuveson DA, Nimsky C, Bartsch JW (2015) ADAM8 as a drug target in pancreatic cancer. Nat Commun. 6: 6175.
13. Amour A, Knight CG, English WR, Webster A, Slocombe PM, Knäuper V, Docherty AJ, Becherer JD, Blobel CP, Murphy G (2002) The enzymatic activity of ADAM8 and ADAM9 is not regulated by TIMPs. FEBS Lett. 524: 154-158.
14. Naus S, Reipschläger S, Wildeboer D, Lichtenthaler SF, Mitterreiter S, Guan Z, Moss ML, Bartsch JW (2006) Identification of candidate substrate for ectodomain shedding by the metalloprotease-disintegrin ADAM8.J Biol Chem 387: 337-346.
15. Fourie AM, Coles F, Moreno V, Karlsson L (2003) Catalytic activity of ADAM8, ADAM15, and MDC-L (ADAM28) on synthetic peptide substrates and in ectodomain cleavage of CD23. J Biol Chem 278: 30469-30477.
16. Moss ML, Rasmussen FH (2007) Fluorescent substrates for the proteinases ADAM17, ADAM10, ADAM8, and ADAM12 useful for high-throughput inhibitor screening. Anal Biochem 366: 144-8.
17. Gomez-Gaviro M, Dominguez-Luis M, Canchado J, Calafat J, Janssen H, Lara-pezzi E, Fourie A, Tugores A, Valenzuela-Fernandez A, Mollinedo F, Sanchez-Madrid F, Diaz-Gonzalez F (2007) Expression and regulation of the metalloproteinase ADAM-8 during human neutrophil pathophysiological activation and its catalytic activity on L-selectin shedding. J. Immunol. 178:

8053-8063.

18. Bartsch JW, Wildeboer D, Koller G, Naus S, Rittger A, Moss ML, Minai Y, Jockusch H (2010) Tumor Necrosis Factor-α (TNF-α) regulates shedding of TNF-a receptor 1 by the Metallopprotease-Disintegrin ADAM8: Evidence for a proteaseregulated feedback loop in neuroprotection. J. Neurosci. 30:12210-12218.
19. Nishimura D, Sakai H, Sato F, Nishimura S, Toyama-Sorimachi N, Bartsch JW (2015) Sehara-Fujisawa A. Roles of ADAM8 in elimination of injured muscle fibers prior to skeletal muscle regeneration. Mech Dev. 135: 58-67.
20. Stöcker W, Bode W (1995) Structural features of a superfamily of zinc-endopeptidases: the metzincins. Curr Opin Struct Biol 5: 383-90.
21. Lichtman AH, Abbas AK (2003) Cellular and molecular immunology. Philadelphia: Saunders. pp: 324-325.
22. Henningsson F, Ding Z, Dahlin JS, Linkevicius M, Carlsson F, Grönvik KO, Hallgren J, Heyman B (2011) IgE-mediated enhancement of CD4+ T cell responses in mice requires antigen presentation by CD11c+ cells and not by B cells. PLoS ONE 6: e2176.
23. Kijimoto-Ochiai S (2002) CD23 (the low-affinity IgE receptor) as a C-type lectin: a multidomain and multifunctional molecule. Cellular and Molecular Life Sciences 59: 648-664.
24. Bonnefoy JY, Plater-Zyberk C, Lecoanet-Henchoz S, Gauchat JF, Aubry JP, Graber P (1996) A new role for CD23 in inflammation. Immunol.17: 418-420.
25. Wheeler DJ, Parveen S, Pollock K, Williams RJ (1998) Inhibition of sCD23 and immunoglobulin E release from human B cells by a metalloproteinase inhibitor, GI 129471.Immunology 95: 105-110.
26. Weskamp G, Ford JW, Sturgill J, Martin S, Docherty AJ, Blobel CP (2006) ADAM10 is a principal 'sheddase' of the low-affinity immunoglobulin E receptor Nat. Immunol. 7: 1293-1298.
27. Pankov R, Yamada KM (2002) Fibronectin at a glance. Journal of Cell Science 115: 3861-3.
28. Williams CM, Engler AJ, Slone RD, Galante LL, Schwarzbauer JE (2008)

Fibronectin expression modulates mammary epithelial cell proliferation during acinar differentiation. Cancer Research 68: 3185-92.

29. Schwinn MK, Peters DM (2009) Functional properties of fibronectin in the trabecular meshwork. Exp Eye Res 88: 689-93.
30. Zack MD, Melton MA, Stock JL, Storer CE, Barve RA, Minnerly JC,Weiss DJ, Stejskal JA, Tortorella MD, Turk JR, Shevlin KM, Malfait AM (2009) Reduced incidence and severity of experimental autoimmune arthritis in mice expressing catalytically inactive A distingrin and metalloprotease 8 (ADAM8). Clin.Exp.Immunol 158: 246-256.
31. Zack MD, Malfait AM, Skepner AP, Yates MP, Griggs DW, Hall T, Hills RL, Alston JT, Nemirovskiy OV, Radabaugh MR, Leone JW, Arner EC, Tortorella MD (2009) ADAM8 isolated human osteoarthritic chondrocytes cleaves fibronectin at Ala271. Arthritis & Rheumatism 9: 2704-2713.
32. Ruel N, Markova DZ, Adams SL, Scanzello C, Cs-Szabo G, Gerard D, Shi P, Anderson G, Zack M, An HS, Chen D, Zhang YJ (2014) Fibronectin fragments and the cleaving enzyme ADAM-8 in the degenerative human intervertebral disc. Spine 39: 1274-9.
33. Anderson DG, Li X, Balian G (2005) A fibronectin fragment alters the metabolism by rabbit intervertevral disc cells in vitro. Spine 30: 1242-6.
34. Hoekstra R, Eskens FA, Verweij J (2001) Matrix metalloproteinase inhibitors: current developments and future perspectives. Oncologist 6: 415-27.
35. Anderson IC, Shipp M, Docherty AJP, Teicher BA (1996) Combination therapy including a gelatinase inhibitor and cytotoxic agent reduces local invasion and metastasis of murine Lewis lung carcinoma. Cancer Res 56: 715-718.
36. Brakebusch C, Fassler R (2005) Beta1 integrin function in vivo: adhesion, migration and more. Cancer Metastasis Rev 24: 403-411.
37. Delespesse G, Sarfati M, Wu CY, Fournier S, Letellier M (1992)The low-affinity receptor for IgE. Immunol 125: 77-97.
38. Hynes RO (1990) Fibronectins. Springer-Verlag Inc 98: 201-216.
39. Sakai T, Johnson KJ, Murozono M, Sakai K, Magnuson MA, Wieloch T, Cronberg

T, Isshiki A, Erickson HP, Fassler R (2001) Plasma fibronectin supports neuronal survival and reduces brain injury following transient focal cerebral ischemia but is not essential for skin-wound healing and hemostasis. Nat. Med 7: 324-330.

40. Buzza MS, Zamurs L, Sun J, Bird CH, Smith AI, Trapani JA, Froelich CJ, Nice EC, Bird PI (2005) Extracellular matrix remodeling by human granzyme B via cleavage of vitronectin, fibronectin, and lamin. J.Biol.Chem 280: 23549-23558.
41. Henry C, Hsia, Mohan R, Siobhan A, Corbett (2014) The fate of internalized α5 integrin is regulated by matrix-capable fibronectin. Journal of surgical research 191: 268-79.
42. Hynes RO (2009) The extracellular matrix: not just pretty fibrils. Science; 326: 1216.
43. Corbett SA, Lee L, Wilson CL, Schwarzbauer JE (1997) Covalent cross-linking of fibronectin to fibrin is required for maximal cell adhesion to a fibronectin-fibrin matrix. J Biol Chem 272: 2499.
44. Leiss M, Beckmann K, Girós A, Costell M, Fässler R (2008) The role of integrin binding sites in fibronectin matrix assembly in vivo. Curr Opin Cell Biol. 20: 502-7.
45. Ruoslahti E (1995) Fibronectin and its alpha5 beta1 integrin receptor in malignancy. Invasion Metastasis 14: 87-97.
46. Lloyd AC (2006) Distinct functions for ERKs? Journal of Biology 5:13.
47. Duhamel S, Hebert J, Gaboury L, Bouchard A, Simon R, Sauter G (2012) Sef downregulation by Ras causes MEK1/2 to become aberrantly nuclear localized leading to polyploidy and neoplastic transformation. Cancer Res 72: 626-35.
48. Inoki K, Li Y, Zhu T, Wu J, Guan KL (2002) TSC2 is phosphorylated and inhibited by Akt and suppresses mTOR signaling. Nat. Cell Biol 4: 648-657.
49. Ghayouri M, Boulware D, Nasir A, Strosberg J, Kvols L, Coppola D (2010) Activation of the serine/theronine protein kinase Akt in enteropancreatic neuroendocrine tumors. Anticancer Res 30: 5063-5067.
50. Streuli C (1999) Extracellular matrix remodelling and cellular differentiation. Curr Opin Cell Biol1 11: 634-640.

9. Summary

From recent studies in different tumor entities it became apparent that the membrane-anchored metalloprotease-disintegrin ADAM8 plays an active role in tumor progression and consequently in patient prognosis. It is therefore desirable to understand the functional role of ADAM8 *in vitro* by characterizing the soluble extracellular part of ADAM8, which is called the ADAM8 ectodomain. The human ectodomain ADAM8 (hEctoA8) protein consists of the prodomain, metalloprotease domain (MP), a disintegrin domain (DIS), a cysteine-rich domain (Cys) and a EGF-like domain (EGF), whilst removal of the prodomain by autocatalysis leads to the active form of hEctoA8. Like the full-length ADAM8, hEctoA8 contains the catalytic consensus sequence HEXXHXXGXXHD in the metalloprotease domain and is therefore predicted to be proteolytically active. Up to now, functional studies on ADAM8 *in vitro* were hampered by the lack of sufficient quantities of folded, biologically active, and purified recombinant forms of hEctoA8. In our study, we successfully purified the recombinant hEctoA8 protein from supernatants of transfected HEK cells. Purified recombinant hEctoA8 containing the catalytic function of ADAM8 can cleave CD23 in cells *in trans* and FN *in vitro*; CD23 cleavage resulted in fragments of 37, 33, 25 and 16 kDa and FN cleavage by recombinant hEctoA8 resulted in 9 fragments, one fragment of 38 kDa contains a RGD motif essential for cell adhesion. Functionally, ADAM8-dependent cell adhesion of pancreatic tumor cells Panc1 was affected by FN cleavage and resulted in reduced cell adhesion. Concomitantly, a decreased expression of integrin α5; was found, whereas cleavage of FN by recombinant hEctoA8 had no effect on the expression levels of integrin β1, and on the activation of p-ERK1/2 and p-Akt.

10. Zusammenfassung

In einer Reihe von klinischen Studien wurde nachgewiesen, dass die membranständige Metalloprotease ADAM8 eine Rolle bei der Tumorprogression spielt und eine erhöhte ADAM8-Expression mit einer verschlechterten Patientenprognose einhergeht. Es ist daher notwendig, die Rolle der ADAM8-Aktivität *in vitro* zu verstehen. In dieser Arbeit sollte daher die lösliche Variante von ADAM8, die Ektodomäne (hEctoA8), aufgereinigt und funktionell charakterisiert warden. Diese besteht aus der Prodomäne, der Metalloprotease-Domäne (MP), der Disintegrin-Domäne (DIS), der Cystein-reichen Domäne (Cys) and der EGF-artigen Domäne (EGF). Die autokatalytische Entfernung der Prodomäne führt zur aktiven Protease. Wie das gesamte ADAM8-Molekül auch, enthält das rekombinanten Protein hEctoA8 die für Metzinkine charakteristische Konsensus-Sequenz "HEXXHXXGXXHD" in der MP-Domäne und sollte daher proteolytische Aktivität besitzen. Bis heute war es nur schwer möglich, funktionelle Studien mit ADAM8 *in vitro* durchzuführen, da nicht genügend rekombinantes Protein mit biologischer Aktivität zur Verfügung stand. In dieser Arbeit wurde das rekombinante humane ADAM8 als hEctoA8 erfolgreich aus Überständen von stabil transfizierten und selektionierten HEK293 Zellen aufgereinigt. Das so gewonnene Protein hEctoA8 besitzt eine hohe katalytische Aktivität und kann in einem FRET-basierten Assay ein Fluoreszenz-gequenchtes Peptid spalten, das der ADAM8-Spaltstelle im niedrig-affinen IgE Rezeptor CD23 nachempfunden ist. Interessanterweise wird auch intaktes membranständiges CD23 von der Oberfläche stabiler CD23-exprimierender Zellen in Fragmente von 37, 33, 25 and 16 kDa abgespalten, womit erstmalig eine Susbtratspaltung in *trans* nachgewiesen wurde. Weiterhin wurden die ADAM8-Spaltstellen für das extrazelluläre Matrixprotein Fibronectin (FN) charakterisiert. Es entstanden dabei 9 FN-Fragmente von unterschiedlichem Molekulargewicht. Ein FN-Fragment mit einem Molekulargewicht

von 38 kDa war dabei besonders interessant, da es so genannte Zellbindungsdomänen sowie ein RGD-Motiv enthält. Durch die ADAM8-abhängige Spaltung dieses Fragments kann man davon ausgehen, dass eine durch FN vermittelte Zelladhäsion verloren gehen sollte. Diese Hypothese wurde durch Pankreas-Tumorzellen Panc1 überprüft, bei denen eine ADAM8-abhängige Zelladhäsion auf FN mit und ohne vorherigen Verdau gemessen wurde. Es konnte gezeigt werden, dass der Verdau von Fibronektin durch ADAM8 die Zelladhäsion signifikant reduzierte. Die Expression des daran beteiligten Fibronektin-Rezeptors $\alpha5\beta1$ wurde auf Proteinebene untersucht und dabei gezeigt, dass spezifisch die Integrin $\alpha5$-Untereinheit vermindert ist, während die Integrin $\beta1$-Untereinheit nicht verändert ist. Auch die vom Fibronektin-Rezeptor abhängige Signalkaskade, an der unter anderem die Kinasen p-ERK1/2 und p-Akt beteiligt sind, zeigt keine Änderungen im Aktivierungsstatus, sodass man daraus schliessen kann, dass die von ADAM8 vermittelte Degradation von FN direkt über die Regulation der Integrin $\alpha5$-Untereinheit zu einer verminderten Zelladhäsion führt.

11. Appendix

11.1 Sequence of Fibronectin Fragments:

FN1(Position: 1035-2386 Predicted MW: 169KD): RGQPR QYNVGPSVSK YPLRNLQPAS EYTVSLVAIK GNQESPKATG VFTTLQPGSS IPPYNTEVTE TTIVITWTPA PRIGFKLGVR PSQGGEAPRE VTSDSGSIVV SGLTPGVEYV YTIQVLRDGQ ERDAPIVNKV VTPLSPPTNL HLEANPDTGV LTVSWERSTT PDITGYRITT TPTNGQQGNS LEEVVHADQS SCTFDNLSPG LEYNVSVYTV KDDKESVPIS DTIIPAVPPP TDLRFTNIGP DTMRVTWAPP PSIDLTNFLV RYSPVKNEED VAELSISPSD NAVVLTNLLP GTEYVVSVSS VYEQHESTPL RGRQKTGLDS PTGIDFSDIT ANSFTVHWIA PRATITGYRI RHHPEHFSGR PREDRVPHSR NSITLTNLTP GTEYVVSIVA LNGREESPLL IGQQSTVSDV PRDLEVVAAT PTSLLISWDA PAVTVRYYRI TYGETGGNSP VQEFTVPGSK STATISGLKP GVDYTITVYA VTGRGDSPAS SKPISINYRT EIDKPSQMQV TDVQDNSISV KWLPSSSPVT GYRVTTTPKN GPGPTKTKTA GPDQTEMTIE GLQPTVEYVV SVYAQNPSGE SQPLVQTAVT NIDRPKGLAF TDVDVDSIKI AWESPQGQVS RYRVTYSSPE DGIHELFPAP DGEEDTAELQ GLRPGSEYTV SVVALHDDME SQPLIGTQST AIPAPTDLKF TQVTPTSLSA QWTPPNVQLT GYRVRVTPKE KTGPMKEINL APDSSSVVVS GLMVATKYEV SVYALKDTLT SRPAQGVVTT LENVSPPRRA RVTDATETTI TISWRTKTET ITGFQVDAVP ANGQTPIQRT IKPDVRSYTI TGLQPGTDYK IYLYTLNDNA RSSPVVIDAS TAIDAPSNLR FLATTPNSLL VSWQPPRARI TGYIIKYEKP GSPPREVVPR PRPGVTEATI TGLEPGTEYT IYVIALKNNQ KSEPLIGRKK TDELPQLVTL PHPNLHGPEI LDVPSTVQKT PFVTHPGYDT GNGIQLPGTS GQQPSVGQQM IFEEHGFRRT TPPTTATPIR HRPRPYPPNV GEEIQIGHIP REDVDYHLYP HGPGLNPNAS TGQEALSQTT ISWAPFQDTS EYIISCHPVG TDEEPLQFRV PGTSTSATLT GLTRGATYNV IVEALKDQQR HKVREEVVTV GNSVNEGLNQ PTDDSCFDPY TVSHYAVGDE WERMSESGFK LLCQCLGFGS GHFRCDSSRW CHDNGVNYKI GEKWDRQGEN GQMMSCTCLG NGKGEFKCDP HEATCYDDGK TYHVGEQWQK EYLGAICSCT CFGGQRGWRC DNCRRPGGEP SPEGTTGQSY NQYSQRYHQR TNTNVNCPIE CFMPLDVQAD REDSRE

FN2(Position: 0-1035 Predicted MW: 129KD): MLRGPGPGLL LLAVQCLGTA VPSTGASKSK RQAQQMVQPQ SPVAVSQSKP GCYDNGKHYQ INQQWERTYL GNALVCTCYG GSRGFNCESK PEAEETCFDK YTGNTYRVGD TYERPKDSMI WDCTCIGAGR GRISCTIANR CHEGGQSYKI GDTWRRPHET GGYMLECVCL GNGKGEWTCK PIAEKCFDHA AGTSYVVGET WEKPYQGWMM VDCTCLGEGS GRITCTSRNR CNDQDTRTSY RIGDTWSKKD NRGNLLQCIC TGNGRGEWKC ERHTSVQTTS SGSGPFTDVR AAVYQPQPHP QPPPYGHCVT DSGVVYSVGM QWLKTQGNKQ MLCTCLGNGV SCQETAVTQT YGGNSNGEPC VLPFTYNGRT FYSCTTEGRQ DGHLWCSTTS NYEQDQKYSF CTDHTVLVQT RGGNSNGALC HFPFLYNNHN YTDCTSEGRR DNMKWCGTTQ NYDADQKFGF CPMAAHEEIC TTNEGVMYRI GDQWDKQHDM GHMMRCTCVG NGRGEWTCIA YSQLRDQCIV DDITYNVNDT FHKRHEEGHM LNCTCFGQGR GRWKCDPVDQ CQDSETGTFY QIGDSWEKYV HGVRYQCYCY GRGIGEWHCQ PLQTYPSSSG PVEVFITETP SQPNSHPIQW NAPQPSHISK YILRWRPKNS VGRWKEATIP GHLNSYTIKG LKPGVVYEGQ LISIQQYGHQ EVTRFDFTTT STSTPVTSNT VTGETTPFSP LVATSESVTE ITASSFVVSW VSASDTVSGF RVEYELSEEG DEPQYLDLPS TATSVNIPDL LPGRKYIVNV YQISEDGEQS LILSTSQTTA PDAPPDTTVD QVDDTSIVVR WSRPQAPITG YRIVYSPSVE GSSTELNLPE TANSVTLSDL QPGVQYNITI YAVEENQEST PVVIQQETTG

TPRSDTVPSP RDLQFVEVTD VKVTIMWTPP ESAVTGYRVD VIPVNLPGEH GQRLPISRNT FAEVTGLSPG VTYYFKVFAV SHGRESKPLT AQQTTKLDAP TNLQFVNETD STVLVRWTPP RAQITGYRLT VGLTR

FN3(Position: 291-1252 Predicted MW: 119KD): AAVYQPQPHP QPPPYGHCVT DSGVVYSVGM QWLKTQGNKQ MLCTCLGNGV SCQETAVTQT YGGNSNGEPC VLPFTYNGRT FYSCTTEGRQ DGHLWCSTTS NYEQDQKYSF CTDHTVLVQT RGGNSNGALC HFPFLYNNHN YTDCTSEGRR DNMKWCGTTQ NYDADQKFGF CPMAAHEEIC TTNEGVMYRI GDQWDKQHDM GHMMRCTCVG NGRGEWTCIA YSQLRDQCIV DDITYNVNDT FHKRHEEGHM LNCTCFGQGR GRWKCDPVDQ CQDSETGTFY QIGDSWEKYV HGVRYQCYCY GRGIGEWHCQ PLQTYPSSSG PVEVFITETP SQPNSHPIQW NAPQPSHISK YILRWRPKNS VGRWKEATIP GHLNSYTIKG LKPGVVYEGQ LISIQQYGHQ EVTRFDFTTT STSTPVTSNT VTGETTPFSP LVATSESVTE ITASSFVVSW VSASDTVSGF RVEYELSEEG DEPQYLDLPS TATSVNIPDL LPGRKYIVNV YQISEDGEQS LILSTSQTTA PDAPPDTTVD QVDDTSIVVR WSRPQAPITG YRIVYSPSVE GSSTELNLPE TANSVTLSDL QPGVQYNITI YAVEENQEST PVVIQQETTG TPRSDTVPSP RDLQFVEVTD VKVTIMWTPP ESAVTGYRVD VIPVNLPGEH GQRLPISRNT FAEVTGLSPG VTYYFKVFAV SHGRESKPLT AQQTTKLDAP TNLQFVNETD STVLVRWTPP RAQITGYRLT VGLTRRGQPR QYNVGPSVSK YPLRNLQPAS EYTVSLVAIK GNQESPKATG VFTTLQPGSS IPPYNTEVTE TTIVITWTPA PRIGFKLGVR PSQGGEAPRE VTSDSGSIVV SGLTPGVEYV YTIQVLRDGQ ERDAPIVNKV VTPLSPPTNL HLEANPDTGV LTVSWERSTT PDITGYRITT TPTNGQQGNS LEEVVHADQS SCTFDNLSPG LEYNVSVYTV KDDKE

FN4(Position: 1506-2386 Predicted MW: 110KD): PGSK STATISGLKP GVDYTITVYA VTGRGDSPAS SKPISINYRT EIDKPSQMQV TDVQDNSISV KWLPSSSPVT GYRVTTTPKN GPGPTKTKTA GPDQTEMTIE GLQPTVEYVV SVYAQNPSGE SQPLVQTAVT NIDRPKGLAF TDVDVDSIKI AWESPQGQVS RYRVTYSSPE DGIHELFPAP DGEEDTAELQ GLRPGSEYTV SVVALHDDME SQPLIGTQST AIPAPTDLKF TQVTPTSLSA QWTPPNVQLT GYRVRVTPKE KTGPMKEINL APDSSSVVVS GLMVATKYEV SVYALKDTLT SRPAQGVVTT LENVSPPRRA RVTDATETTI TISWRTKTET ITGFQVDAVP ANGQTPIQRT IKPDVRSYTI TGLQPGTDYK IYLYTLNDNA RSSPVVIDAS TAIDAPSNLR FLATTPNSLL VSWQPPRARI TGYIIKYEKP GSPPREVVPR PRPGVTEATI TGLEPGTEYT IYVIALKNNQ KSEPLIGRKK TDELPQLVTL PHPNLHGPEI LDVPSTVQKT PFVTHPGYDT GNGIQLPGTS GQQPSVGQQM IFEEHGFRRT TPPTTATPIR HRPRPYPPNV GEEIQIGHIP REDVDYHLYP HGPGLNPNAS TGQEALSQTT ISWAPFQDTS EYIISCHPVG TDEEPLQFRV PGTSTSATLT GLTRGATYNV IVEALKDQQR HKVREEVVTV GNSVNEGLNQ PTDDSCFDPY TVSHYAVGDE WERMSESGFK LLCQCLGFGS GHFRCDSSRW CHDNGVNYKI GEKWDRQGEN GQMMSCTCLG NGKGEFKCDP HEATCYDDGK TYHVGEQWQK EYLGAICSCT CFGGQRGWRC DNCRRPGGEP SPEGTTGQSY NQYSQRYHQR TNTNVNCPIE CFMPLDVQAD REDSRE

FN5(Position: 1656-2386 Predicted MW: 91KD): TDVDVDSIKI AWESPQGQVS RYRVTYSSPE DGIHELFPAP DGEEDTAELQ GLRPGSEYTV SVVALHDDME SQPLIGTQST AIPAPTDLKF TQVTPTSLSA QWTPPNVQLT GYRVRVTPKE KTGPMKEINL APDSSSVVVS GLMVATKYEV SVYALKDTLT SRPAQGVVTT LENVSPPRRA RVTDATETTI TISWRTKTET ITGFQVDAVP ANGQTPIQRT IKPDVRSYTI TGLQPGTDYK IYLYTLNDNA RSSPVVIDAS TAIDAPSNLR FLATTPNSLL VSWQPPRARI TGYIIKYEKP GSPPREVVPR PRPGVTEATI TGLEPGTEYT IYVIALKNNQ KSEPLIGRKK TDELPQLVTL PHPNLHGPEI LDVPSTVQKT PFVTHPGYDT GNGIQLPGTS GQQPSVGQQM IFEEHGFRRT TPPTTATPIR HRPRPYPPNV

GEEIQIGHIP REDVDYHLYP HGPGLNPNAS TGQEALSQTT ISWAPFQDTS EYIISCHPVG TDEEPLQFRV PGTSTSATLT GLTRGATYNV IVEALKDQQR HKVREEVVTV GNSVNEGLNQ PTDDSCFDPY TVSHYAVGDE WERMSESGFK LLCQCLGFGS GHFRCDSSRW CHDNGVNYKI GEKWDRQGEN GQMMSCTCLG NGKGEFKCDP HEATCYDDGK TYHVGEQWQK EYLGAICSCT CFGGQRGWRC DNCRRPGGEP SPEGTTGQSY NQYSQRYHQR TNTNVNCPIE CFMPLDVQAD REDSRE

FN6(Position: 1285-1575 Predicted MW: 38KD): RVTWAPP PSIDLTNFLV RYSPVKNEED VAELSISPSD NAVVLTNLLP GTEYVVSVSS VYEQHESTPL RGRQKTGLDS PTGIDFSDIT ANSFTVHWIA PRATITGYRI RHHPEHFSGR PREDRVPHSR NSITLTNLTP GTEYVVSIVA LNGREESPLL IGQQSTVSDV PRDLEVVAAT PTSLLISWDA PAVTVRYYRI TYGETGGNSP VQEFTVPGSK STATISGLKP GVDYTITVYA VTGRGDSPAS SKPISINYRT EIDKPSQMQV TDVQDNSISV KWLPSSSPVT GYR

FN7(Position: 1940-2180 Predicted MW: 31KD): TGYIIKYEKP GSPPREVVPR PRPGVTEATI TGLEPGTEYT IYVIALKNNQ KSEPLIGRKK TDELPQLVTL PHPNLHGPEI LDVPSTVQKT PFVTHPGYDT GNGIQLPGTS GQQPSVGQQM IFEEHGFRRT TPPTTATPIR HRPRPYPPNV GEEIQIGHIP REDVDYHLYP HGPGLNPNAS TGQEALSQTT ISWAPFQDTS EYIISCHPVG TDEEPLQFRV PGTSTSATLT GLTRGATYNV

FN8(Position: 881-1073 Predicted MW: 22.4KD): YAVEENQEST PVVIQQETTG TPRSDTVPSP RDLQFVEVTD VKVTIMWTPP ESAVTGYRVD VIPVNLPGEH GQRLPISRNT FAEVTGLSPG VTYYFKVFAV SHGRESKPLT AQQTTKLDAP

FN9(Position: 0-109 Predicted MW: 12KD): MLRGPGPGLL LLAVQCLGTA VPSTGASKSK RQAQQMVQPQ SPVAVSQSKP GCYDNGKHYQ INQQWERTYL GNALVCTCYG GSRGFNCESK PEAEETCFDK YTGNTYRVGD TYERPK

11.2 Acknowledgments

First of all, I want to show my great appreciation to my supervisor, **Prof. Dr. Jörg W. Bartsch**, for his enthusiastic support, patient education, constructive comments, intensive theoretical discussions and intellectual guidance he extended me throughout my study. I am also greatly grateful to him for the correction and critical comments in reviewing and revising the manuscript of this thesis and his friendly company and continuous encouragement throughout my study saving no effort. I also should thank **Dr. Uwe Schlomann** for his kind-hearted help, he helped me to constructed cell lines that I used for my experiments and he taught me the skills required for the experiments and instructed me every detail during my dissertation research, I could not have finished my research without his help.

I thank **PD Dr. Oliver Schilling**, Freiburg University, for analysis of FN fragments by Mass Spectrometry analysis.

I am also very grateful to **Prof. Dr. Ch. Nimsky** who gave me the opportunity to finish my study at the Faculty of Medicine of Philipps-University Marburg.

My special thanks should go to **Songbo Guo, Sabine Motzny, Cathi Conrad** and **Junweng Wang** for their help.

I also thank my family and my hospital for their support.